The Internet of Things in Oil/Gas Reservoir

Dr. Abdallah A. Alshehri

EXPEC Advanced Research Center (EXPEC ARC)
Saudi Aramco, Saudi Arabia

abdullah.shehri.8@aramco.com

October 18-22, 2020

IoT in Upstream Oil / Gas

Upstream Operations:

- Exploration
- Drilling
- Completions
- Production
- Logging and Intervention
- Real-time Monitoring & Control

Sensing Applications:

- ✓ Seismic
- ✓ Signal processing
- ✓ MWD & LWD
- ✓ Remote Sensing
- ✓ Geo-steering
- ✓ Microchips
- ✓ Autonomous rigs
- ✓ Water front detection
- ✓ I-field

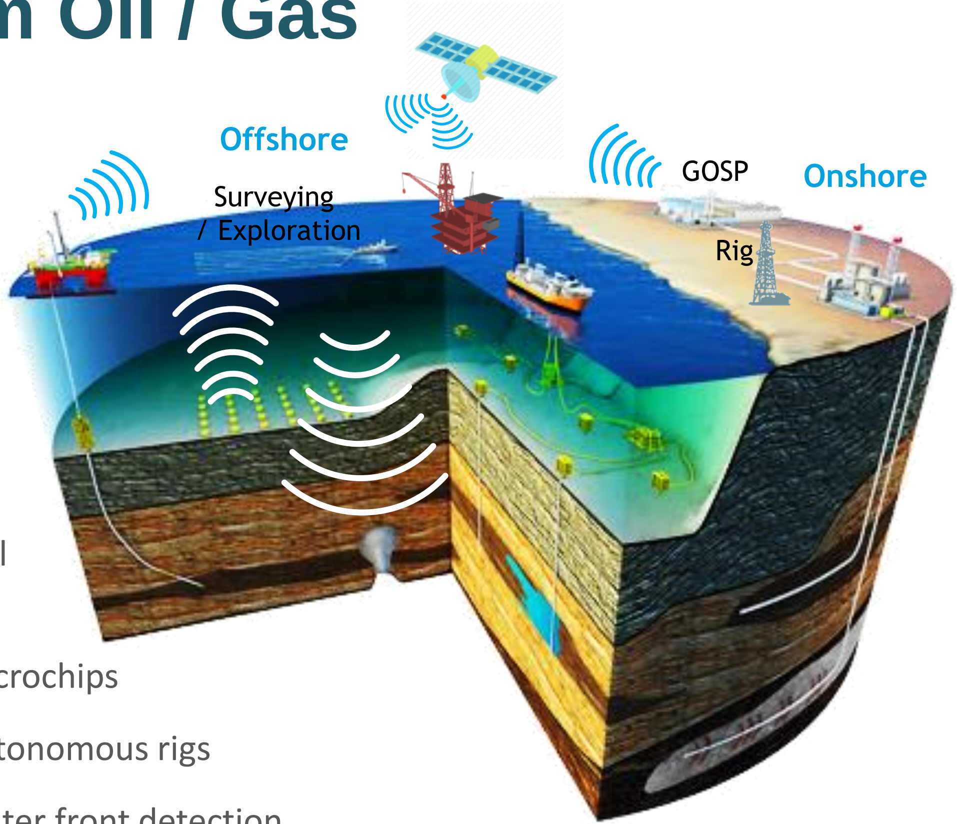

*Picture Courtesy of: http://www.bouncingpixel.com

Hydraulic Fractures

- Hydraulic Fractures are formed by pumping a fluid into the wellbore at a rate sufficient to increase the pressure downhole in order to crack the formation.

- Access unconventional oil and gas reservoirs
- Access tight conventional gas reservoirs
- Improve reservoir contact and production rates

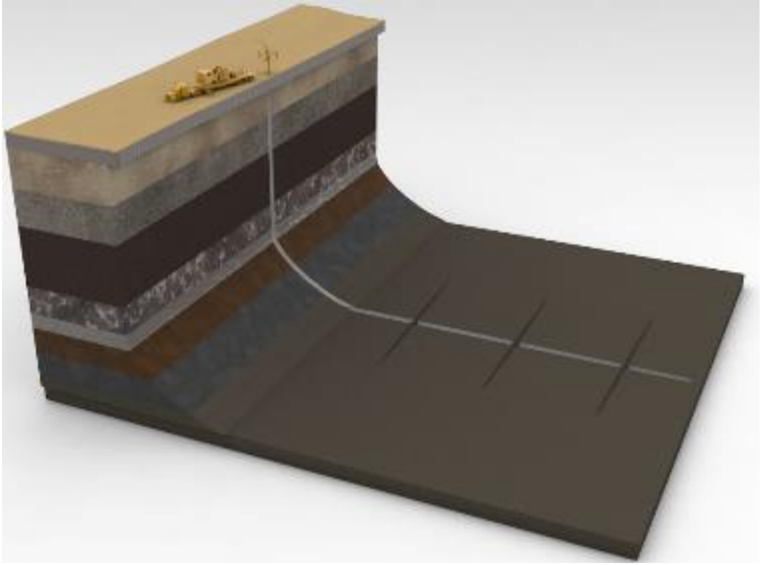

Field Challenges

- Uncertainty in fracture mapping
- Conceptual fracture models
- Lack of dynamic stress data

Business Impact

- Optimize fracturing jobs
- Maximize well productivity
- Maximize hydrocarbon recovery

What Are FracBots?

- Tiny devices (IoT) with wireless communication, localization and sensing capabilities

- Real-time mapping of fracture networks

- Real-time reservoir information

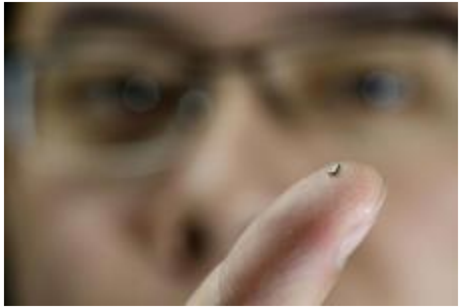

How FracBots Technology Works

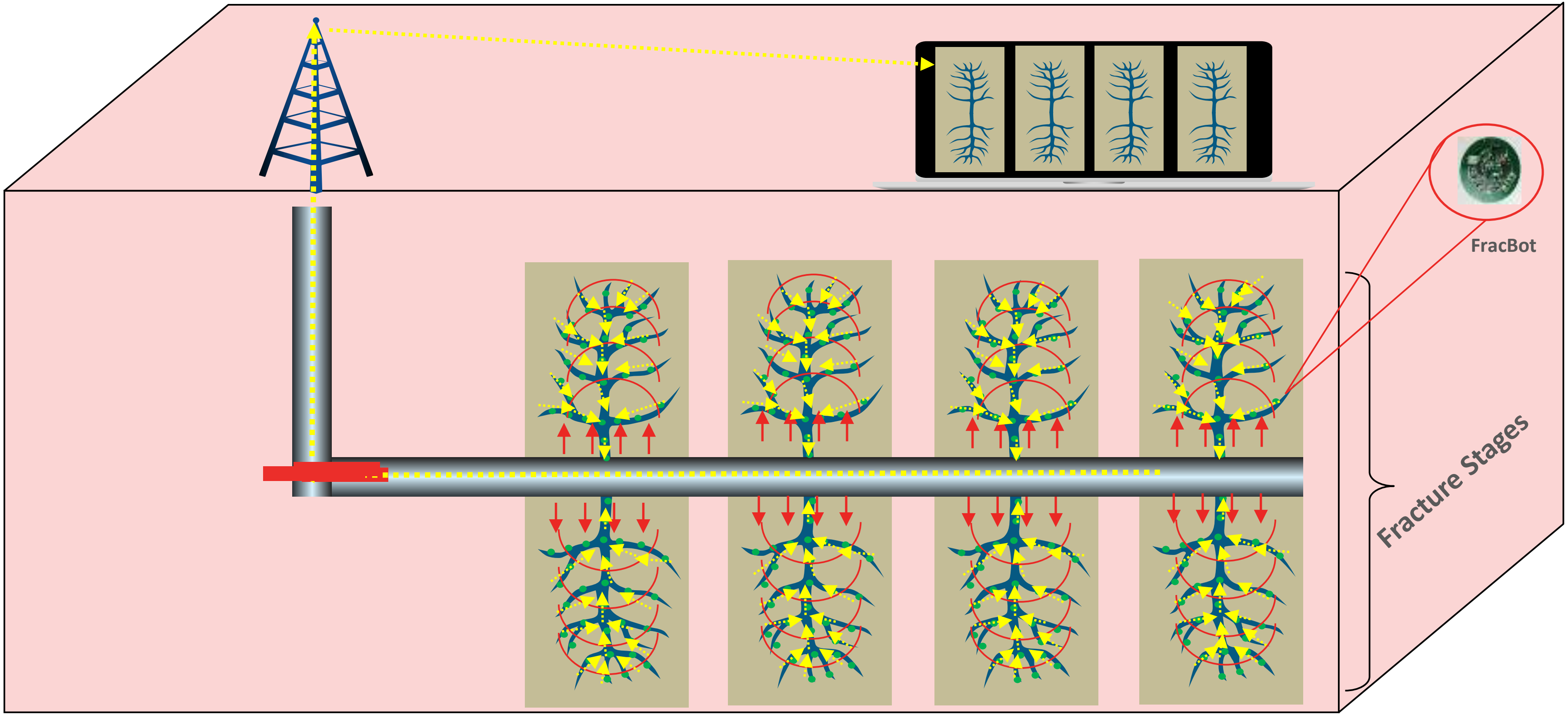

Hydraulic Fractures Environment Challenges

- Deploy and operate FracBots as a Wireless Sensor Network (WSN) in a fracture.

- Key challenges:
  - High path loss
  - Difficulty in launching wireless signals
  - Short system lifetime
  - Small device size
  - Energy-Limited Environment

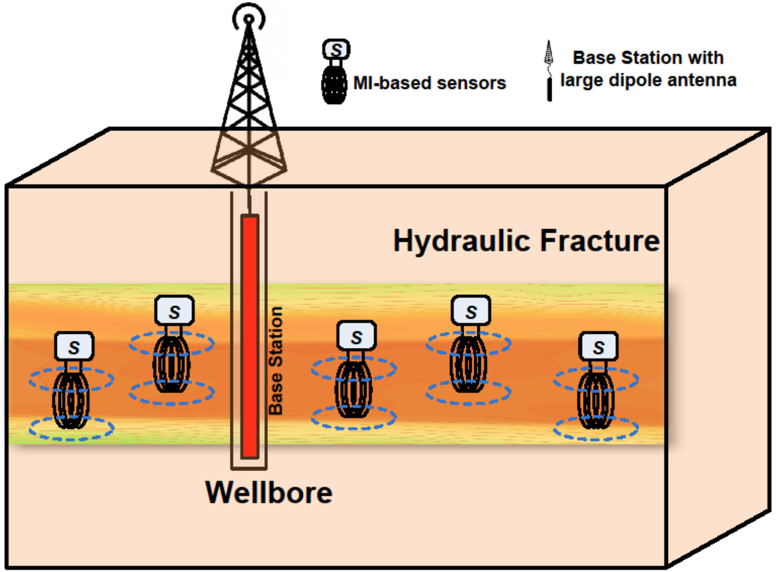

Wireless Communication Techniques

• Electromagnetic waves (EM)

❖ Classical EM waves cannot work properly in the underground oil reservoir environment.

❑ **The main problems of EM :**

1. Extremely short communication ranges due to high path loss
2. Highly unreliable channel conditions
3. Large antenna size since the path loss of low frequency signal is small.

• Magnetic Induction (MI)

❖ MI utilizes the time-varying near magnetic field to propagate the information.

❑ **The main advantages of MI :**

1. Highly reliable and constant channel conditions.
2. The multi-path fading is negligible in underground MI communication because the communication range is within one wavelength.
3. A small size wire coil.
4. There is no cutoff frequency.

Key Challenges

- A Structural dimension of the fracture, the structural constrain demands ultra-scaled standalone system development.
- The harsh environment consisting of crude oil, gas, soil and rocks and other injection fluids, causes high path loss for effective communication.
- Limited power supply in the harsh environment
- Scale down the node to smaller size.
- Unavailable of electronic components that can serve the size reduction.
- Unavailable of electronic components that can sustain high temperature and pressure.

MI Channel Model in Hydraulic Fractures

HF Network Topology

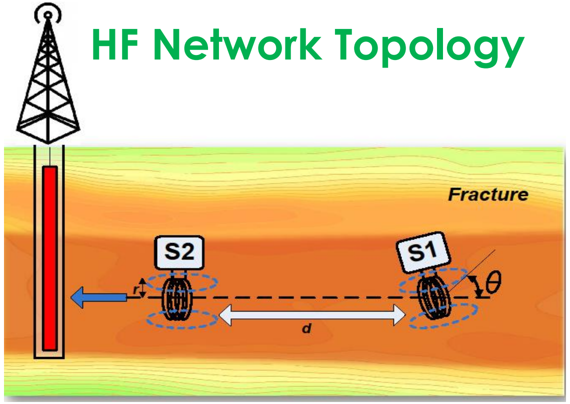

The equivalent circuit

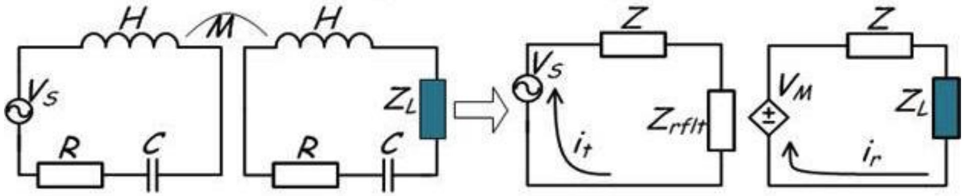

Transformer model of a MI transceiver.

Sensing Unit

- Temperature *T*
- Electric Conductivity *σ*

- Magnetic Permeability *μ*
- Coil Resistance *R*

MI Communication

Path Loss L_{MI}

Channel Bandwidth B_{MI}

$$L_{MI}(r, f_0, \theta, T, \sigma)\ [\text{dB}] = 10 \lg \frac{2(2R^2 + \omega_0^2 M^2)}{\omega_0^2 M^2} \approx 10 \lg \frac{4R^2}{\omega_0^2 M^2} \triangleq 10 \lg \frac{1}{\varepsilon(r, f_0, \theta, T, \sigma)}$$

Performance Evaluation: Frequency Response & Path loss

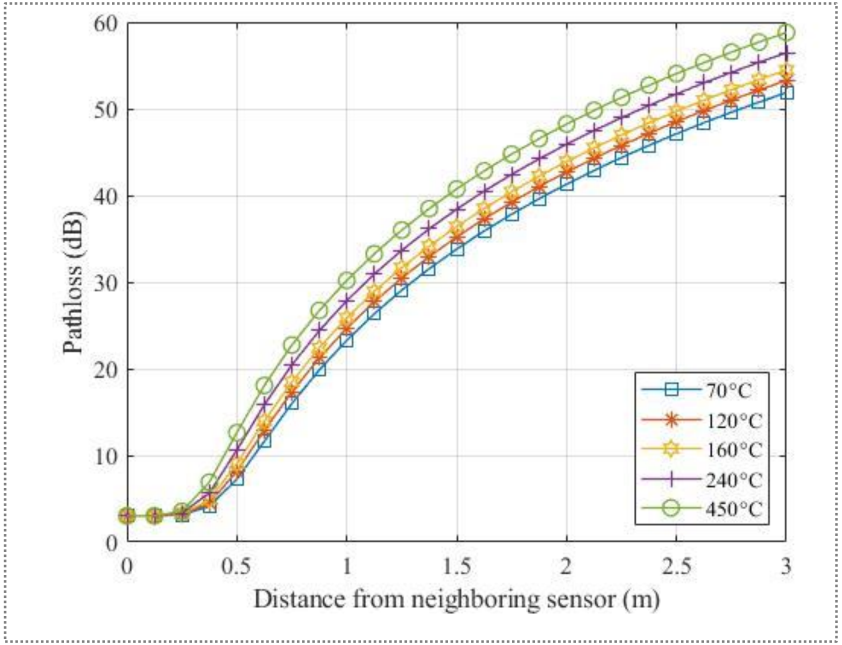

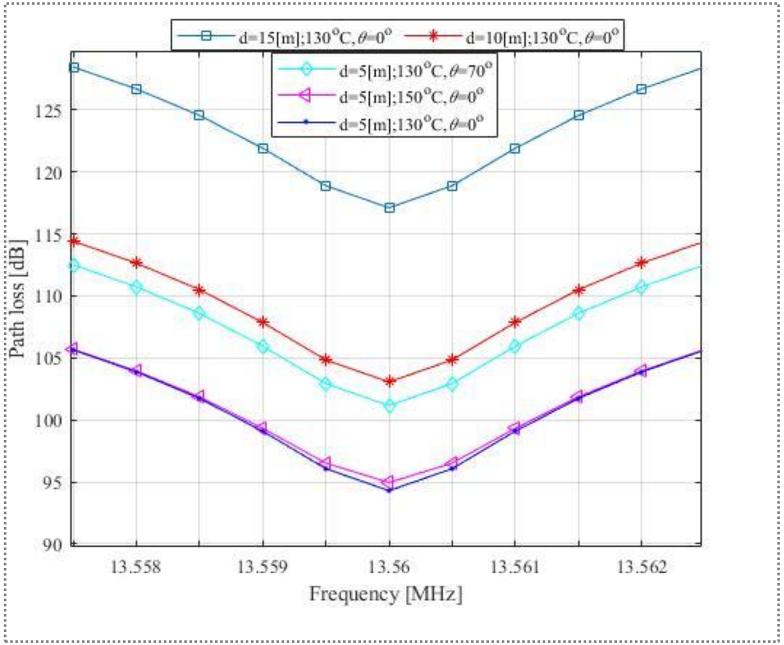

Path loss of magnetic induction at different hydraulic fracture temperatures

MI channel responses at various communication ranges, temperatures and alignment angles

Comparison of the path loss in EM and MI

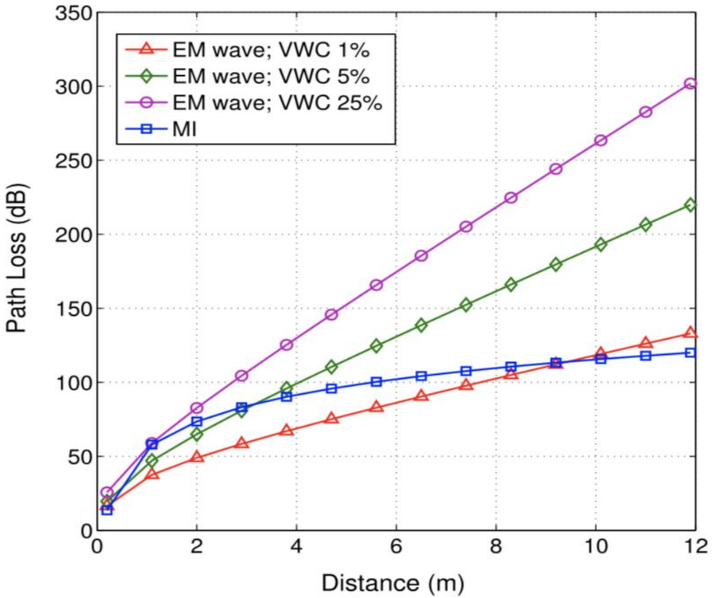

Compares the path loss in EM and MI communications. While the EM path loss intensely increases as VWC increases, the MI path loss is not impacted as the volumetric water content increases. However, when VWC is 1% (dry soil), the EM path loss is smaller than that in the MI system. It means that EM is better to be used for short ranges but at controlled environment with less conductivity.

FracBots Components

Software Development

- Cross-layer Communication
- Localization Algorithms
- Energy Management

FracBot

Hardware Design

- Magnetic Antenna
- Microprocessor
- Energy Harvesting Unit

Gen I R&D Milestones

1. Cross-layer Communication

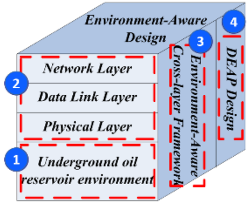

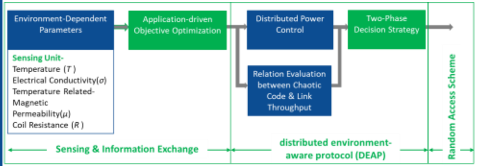

Algorithm 1 Distributed Cross-layer Link Optimization

Input: $i, j, r_{ij}, \theta_{ij}$

$EaT_{min} = \infty$ % Initialization
for $mod = 1 : |M|$ **do** % Modulation cycle
  for $fec = 1 : |C|$ **do** % FEC cycle
    Calculate r^{j}_{min} via tolerable end-to-end PER Φ^{e2e}_{T}
    $(EaT_{ij}, P, Q, l) \leftarrow$ **Algorithm** 2$(r^{j}_{min}, NI_j, r_{ij}, \theta_{ij},$
      $m_{ij}(mod), c_{ij}(fec))$
    if $EaT_{ij} < EaT_{min}$ **then**
      $EaT_{min} = EaT_{ij}$
      $(m, c, P, Q, l)^* = (m(mod), c(fec), P, Q, l)$

Patented in US office

2. FractBots Localization

- RMFS measurements
- Localization Framework
- Fast initial positioning
- Fine-grained positioning

3. Optimal Energy Planning

- Power constraints
- Energy Model framework
- FracBot transmission rates
- FracBot network topology

4. FracBots Design & Testbed

- MI-based FracBot node design
- MI-based FracBot network
- Experimental MI-based testbed

Gen I R&D Milestones

1. Cross-layer Communication

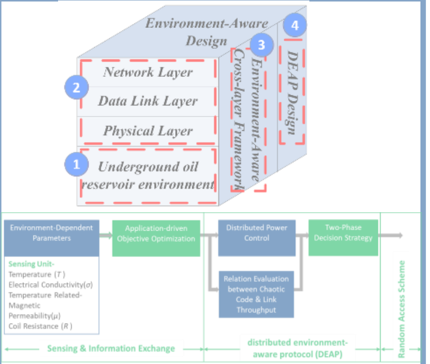

Algorithm 1 Distributed Cross-layer Link Optimization

Input: $i, j, r_{ij}, \theta_{ij}$

1: $EaT_{min} = \infty$ % Initialization
2: **for** $mod = 1 : |\mathcal{M}|$ **do** % Modulation cycle
3: **for** $fec = 1 : |C|$ **do** % FEC cycle
4: **Calculate** r^j_{min} via tolerable end-to-end PER Φ^{e2e}_T
5: $(EaT_{ij}, P, Q, l) \leftarrow$ **Algorithm** 2$(r^j_{min}, NI_j, r_{ij}, \theta_{ij},$
6: $m_{ij}(mod), c_{ij}(fec))$
7: **if** $EaT_{ij} < EaT_{min}$ **then**
8: $EaT_{min} = EaT_{ij}$
9: $(m, c, P, Q, l)^* = (m(mod), c(fec), P, Q, l)$

Patented in US office

2. FractBots Localization

- RMFS measurements
- Localization Framework
- Fast initial positioning
- Fine-grained positioning

3. Optimal Energy Planning

- Power constraints
- Energy Model framework
- FracBot transmission rates
- FracBot network topology

4. FracBots Design & Testbed

- MI-based FracBot node design
- MI-based FracBot network
- Experimental MI-based testbed

Gen I R&D Milestones

1. Cross-layer Communication

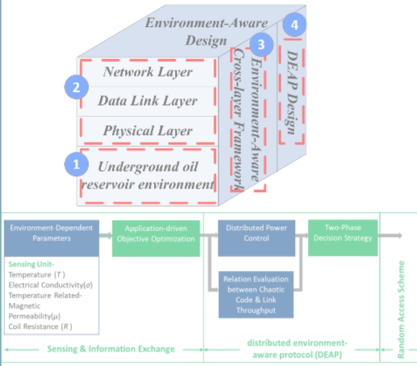

Algorithm 1 Distributed Cross-layer Link Optimization

Input: i, j, r_{ij}, θ_{ij}

1: $EaT_{min} = \infty$ % Initialization
2: **for** $mod = 1 : |\mathcal{M}|$ **do** % Modulation cycle
3: **for** $fec = 1 : |\mathcal{C}|$ **do** % FEC cycle
4: **Calculate** r^{j}_{min} via tolerable end-to-end PER Φ^{e2e}_{T}
5: $(EaT_{ij}, P, Q, l) \leftarrow$ **Algorithm** 2$(r^{j}_{min}, NI_j, r_{ij}, \theta_{ij}, m_{ij}(mod), c_{ij}(fec))$
7: **if** $EaT_{ij} < EaT_{min}$ **then**
8: $EaT_{min} = EaT_{ij}$
9: $(m, c, P, Q, l)^* = (m(mod), c(fec), P, Q, l)$

Patented in US office

2. FractBots Localization

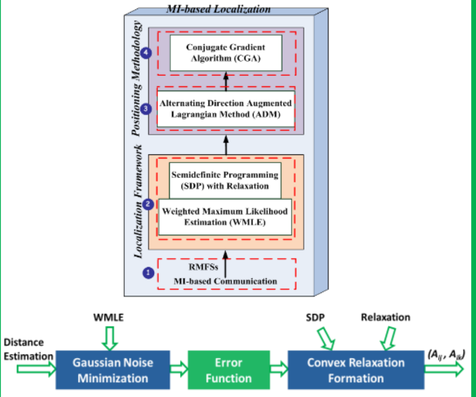

Algorithm 2 CGA (Fine-Grained Positioning)

Input: $f(\cdot)$, $X^{(0)} := [x_1^T, \ldots, x_N^T]^T$ from **Algorithm 1**

Output: X^* % Sensor location **Set** $m = 0$; **compute** $d^{(0)} = -\nabla f(X^{(0)})$

while $\nabla f(X^{(m)}) \neq \mathbf{0}$ **do** **Compute** α_m
Compute $X^{(m+1)}$
Compute β_m
Compute $d^{(m+1)}$
Set $m = m + 1$
end while **Set** $X^* = X^{(m)}$

Patented in US office

3. Optimal Energy Planning

- Power constraints
- Energy Model framework
- FracBot transmission rates
- FracBot network topology

4. FracBots Design & Testbed

- MI-based FracBot node design
- MI-based FracBot network
- Experimental MI-based testbed

Gen I R&D Milestones

1. Cross-layer Communication

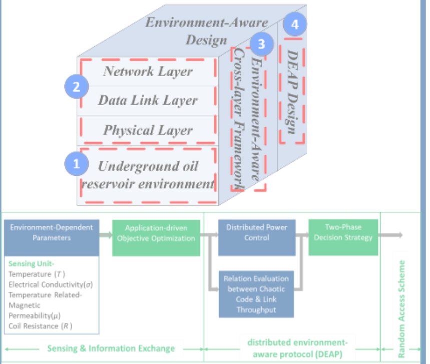

Algorithm 1 Distributed Cross-layer Link Optimization

Input: $i, j, r_{ij}, \theta_{ij}$

1: $EaT_{min} = \infty$ % Initialization
2: **for** $mod = 1 : |\mathcal{M}|$ **do** % Modulation cycle
3: **for** $fec = 1 : |\mathcal{C}|$ **do** % FEC cycle
4: **Calculate** r^{j}_{min} via tolerable end-to-end PER Φ^{e2e}_{T}
5: $(EaT_{ij}, P, Q, l) \leftarrow$ **Algorithm 2**$(r^{j}_{min}, NI_j, r_{ij}, \theta_{ij}, m_{ij}(mod), c_{ij}(fec))$
7: **if** $EaT_{ij} < EaT_{min}$ **then**
8: $EaT_{min} = EaT_{ij}$
9: $(m, c, P, Q, l)^* = (m(mod), c(fec), P, Q, l)$

Patented in US office

2. FractBots Localization

Algorithm 2 CGA (Fine-Grained Positioning)

Input: $f(\cdot)$, $X^{(0)} := [x_1^T, \ldots, x_N^T]^T$ from **Algorithm 1**

Output: X^* % Sensor location **Set** $m = 0$; **compute** $d^{(0)} = -\nabla f(X^{(0)})$

while $\nabla f(X^{(m)}) \neq 0$ **do Compute** α_m
Compute $X^{(m+1)}$
Compute β_m
Compute $d^{(m+1)}$
Set $m = m + 1$
end while**Set** $X^* = X^{(m)}$

Patented in US office

3. Optimal Energy Planning

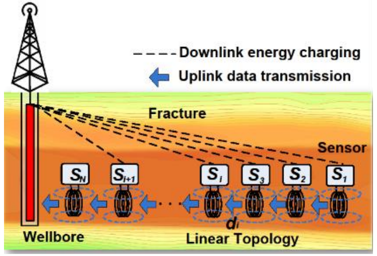

Algorithm 1 Fast Optimal Energy Planning.

set $N = 1$
repeat
calculate
$\lambda^N = \min_{i \leq N} E^h_i / [iR^C(E^{MI}_b(d) + 2E^{elec}_b)]$
set $N := N + 1$
until $N > \log_{(1-\Phi(d))}(1 - \Phi^{e2e}_T)$
$N^* = \arg\max_i i\lambda^i$ and $\lambda^* = \lambda^{N^*}$

Published in IEEE ICC Conference

4. FracBots Design & Testbed

- MI-based FracBot node design
- MI-based FracBot network
- Experimental MI-based testbed

Gen I R&D Milestones

1. Cross-layer Communication

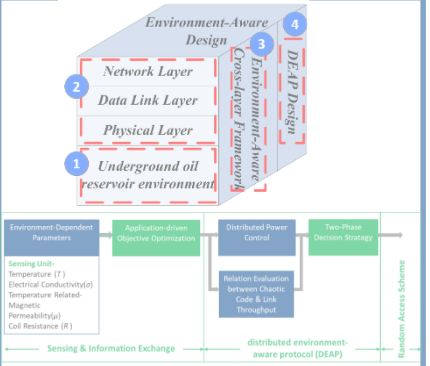

Algorithm 1 Distributed Cross-layer Link Optimization

Input: $i, j, r_{ij}, \theta_{ij}$

$EaT_{min} = \infty$ % Initialization
for $mod = 1 : |\mathcal{M}|$ **do** % Modulation cycle
  for $fec = 1 : |\mathcal{C}|$ **do** % FEC cycle
    Calculate r^j_{min} via tolerable end-to-end PER Φ^{e2e}_T
    $(EaT_{ij}, P, Q, l) \leftarrow$ **Algorithm** 2$(r^j_{min}, NI_j, r_{ij}, \theta_{ij}, m_{ij}(mod), c_{ij}(fec))$
    if $EaT_{ij} < EaT_{min}$ **then**
      $EaT_{min} = EaT_{ij}$
      $(m, c, P, Q, l)^* = (m(mod), c(fec), P, Q, l)$

Patented in US office

2. FractBots Localization

Algorithm 2 CGA (Fine-Grained Positioning)

Input: $f(\cdot)$, $X^{(0)} := [x_1^T, \ldots, x_N^T]^T$ from **Algorithm 1**
Output: X^* % Sensor location **Set** $m = 0$; **compute** $d^{(0)} = -\nabla f(X^{(0)})$
while $\nabla f(X^{(m)}) \neq 0$ **do Compute** α_m
Compute $X^{(m+1)}$
Compute β_m
Compute $d^{(m+1)}$
Set $m = m + 1$
end whileSet $X^* = X^{(m)}$

Patented in US office

3. Optimal Energy Planning

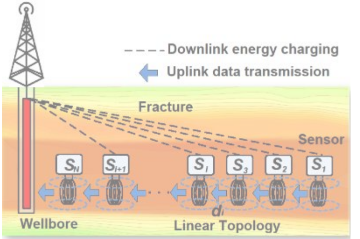

Algorithm 1 Fast Optimal Energy Planning.

set $N = 1$
repeat
  calculate
  $\lambda^N = \min_{i \leq N} E^h_i / [iR^C(E^{MI}_b(d) + 2E^{elec}_b)]$
  set $N := N + 1$
until $N > \log_{(1-\Phi(d))}(1 - \Phi^{e2e}_T)$
$N^* = \arg\max_i i\lambda^i$ and $\lambda^* = \lambda^{N^*}$

Published in IEEE ICC Conference

4. FracBots Design & Testbed

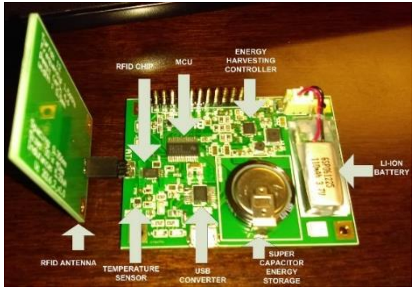

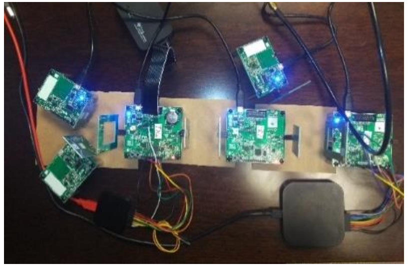

Published in IEEE UEMCON & IEEE SAS Conferences

Gen I R&D Milestones

1. Cross-layer Design

- Evaluate the environment data
- Three-layer protocol
- Cross-layer framework
- Distributed Environment-Aware Protocol

2. FractBots Localization

- RMFS measurements
- Localization Framework
- Fast initial positioning
- Fine-grained positioning

3. Optimal Energy Planning

- Power constraints
- Energy Model framework
- FracBot transmission rates
- FracBot network topology

4. FracBots Design & Testbed

- MI-based FracBot node design
- MI-based FracBot network
- Experimental MI-based testbed

Cross-layer Environment-Aware Protocol Design

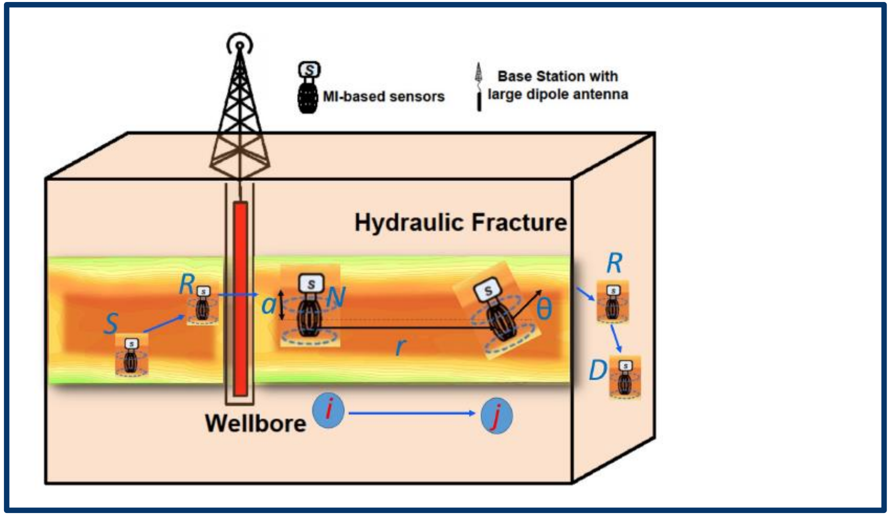

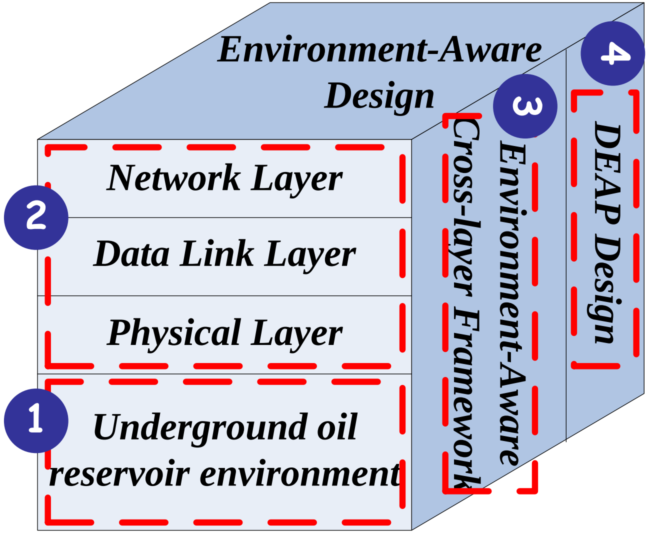

- Evaluation of for the critical environment information of underground oil reservoirs that affects the transmission qualities MI-based communications.
- Three-layer protocol stack for WUSNs in underground oil reservoirs.
- Cross-layer framework to jointly optimize the communication functionalities of different layers.
- Distributed Environment-Aware Protocol (DEAP) design to solve the proposed cross-layer framework.

Cross-layer Design For MI Communication

- Major contributions:

1. Evaluation for the critical environment information of underground oil reservoirs that affects the transmission qualities of MI-based communications.
2. Three-layer protocol stack for WUSNs in underground oil reservoirs.
3. Cross-layer framework to jointly optimize the communication functionalities of different layers.
4. Distributed Environment-Aware Protocol (DEAP) design to solve the proposed cross-layer framework.

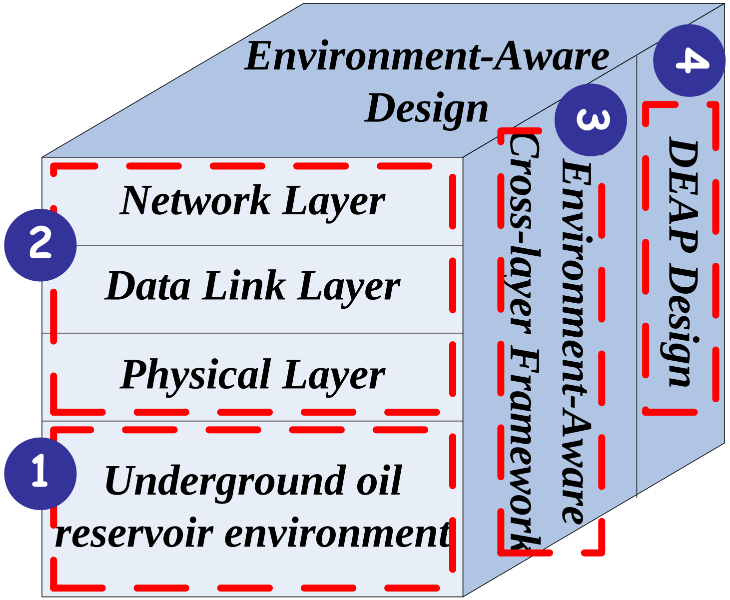

Distributed Environment-Aware Protocol (DEAP) design

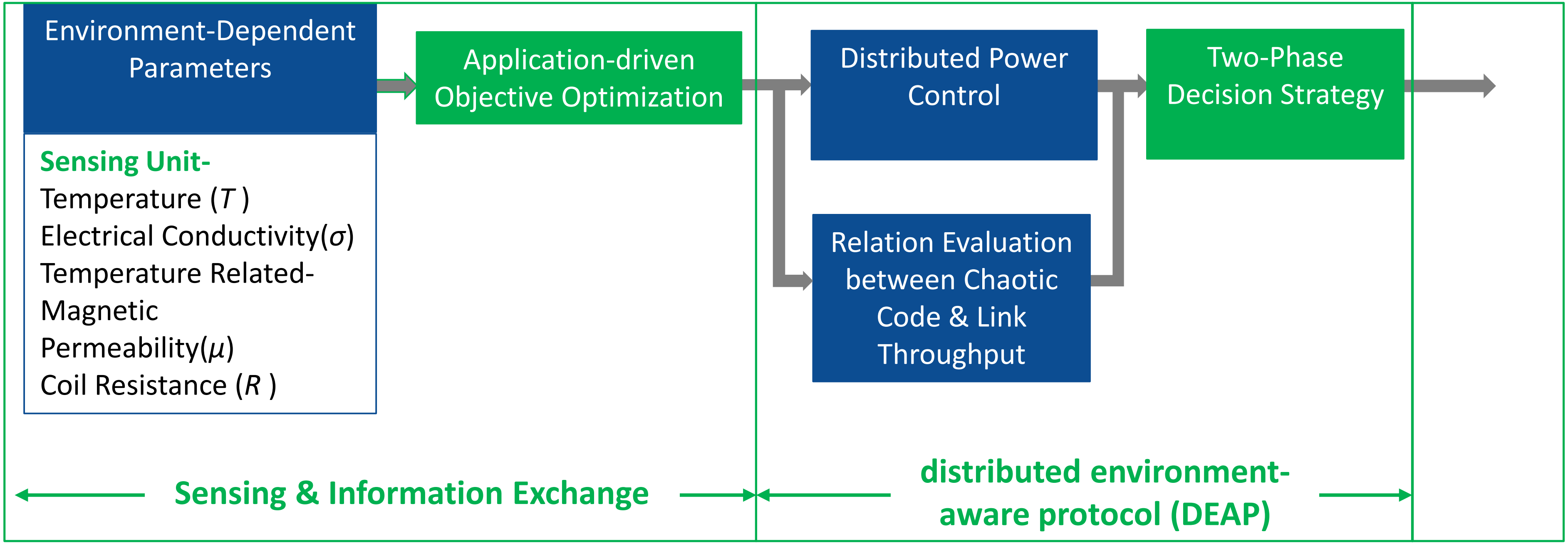

Performance Evaluation: modulation and channel Coding

❑ Schemes:

- Several simple and suitable modulation schemes: BPSK, BFSK, DBPSK, and 16-QAM
- The channel coding schemes: BCH(n, k, t) code

❑ Evaluation parameters:

✓ The transmission range: 7 m
✓ The packet length: 100 Bytes
✓ The working temperature: 283 K

❑ Results:

➢ While BPSK achieves smaller PER for any given SNR among modulation techniques, it brings the best PER performance for every channel coding schemes.
➢ While consuming more energy to perform, the powerful coding schemes keep less PER for any given SNR.
➢ A trade-off exists between energy consumption and transmission quality.

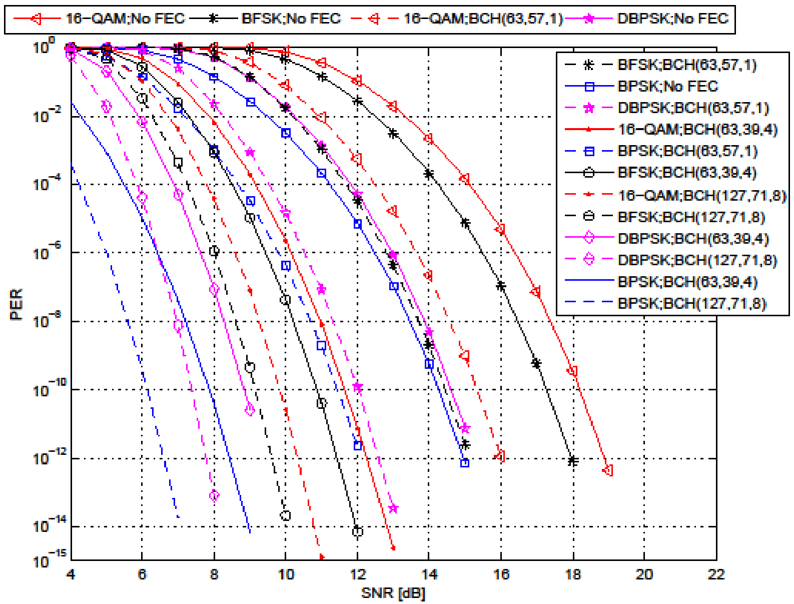

Packet error rate (PER) vs. SNR for typical underground modulation techniques and BCH(n, k, t) coding schemes.

Performance Evaluation: Link Transmissions

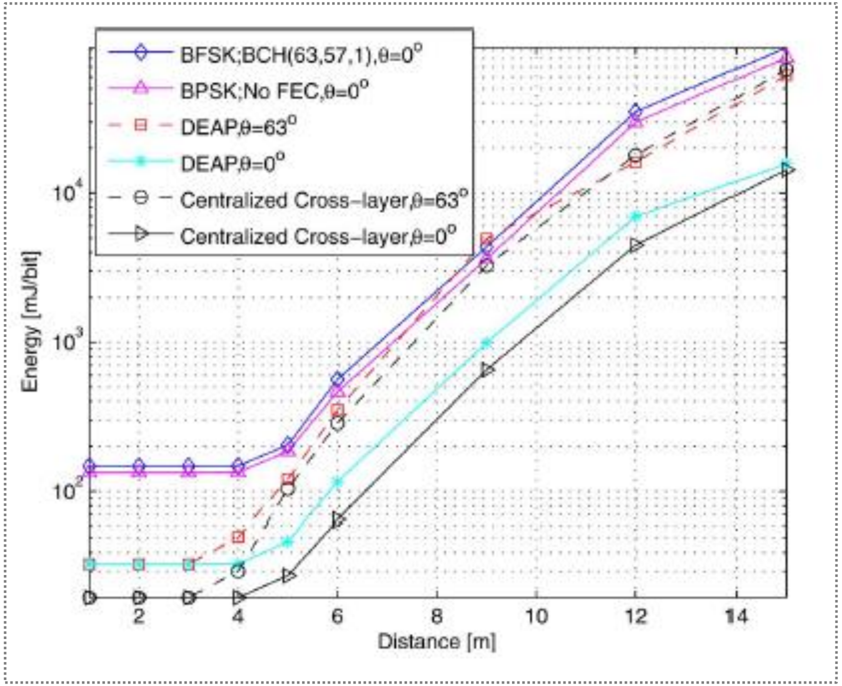

Energy per bit for the centralized cross-layer solution, the cross-layer DEAP, and two fixed modulation/FEC combinations.

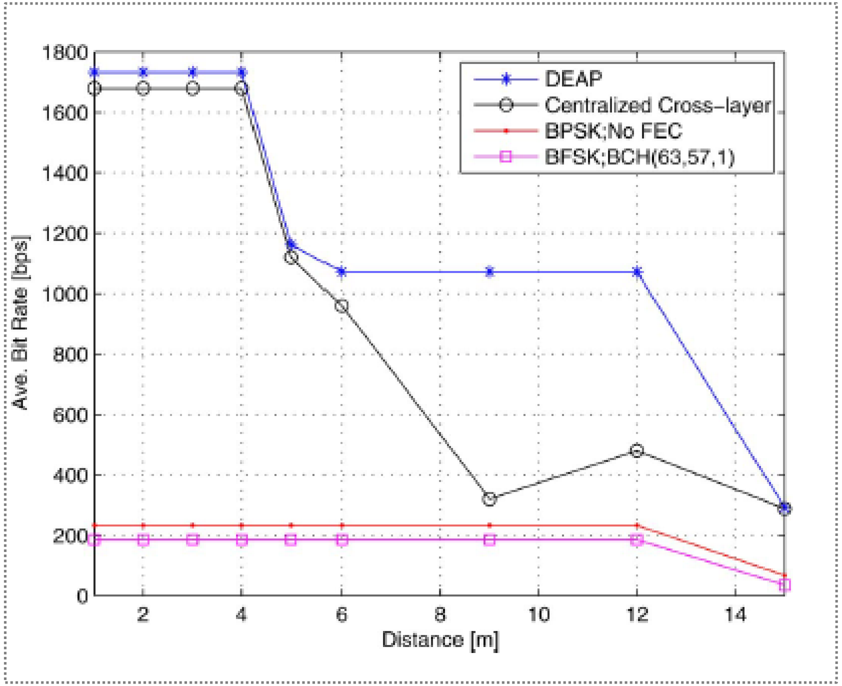

Average bit rate for the centralized cross-layer solution, the cross-layer DEAP, and two fixed modulation/FEC combinations.

Performance Evaluation: End to End Flow

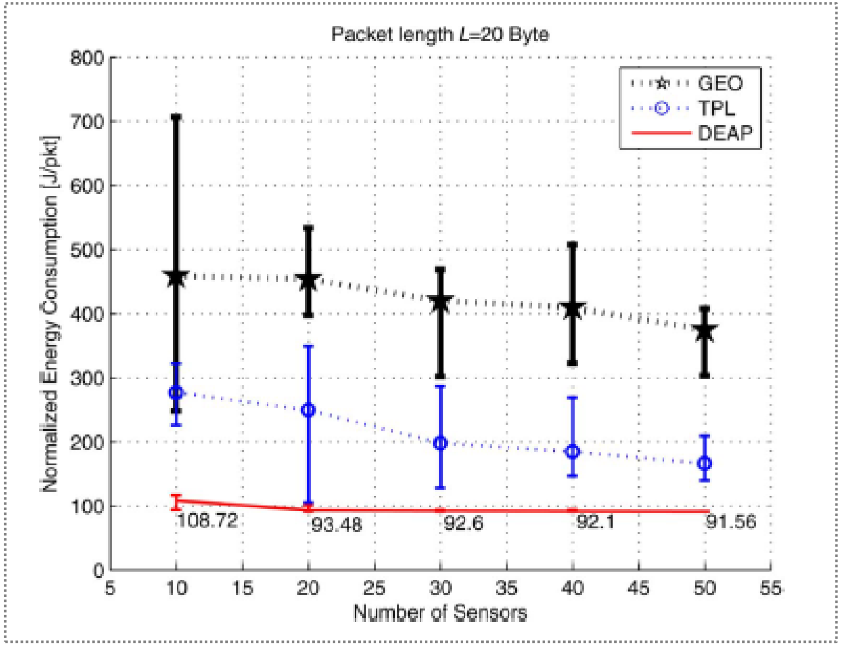

Normalized energy consumption for the cross-layer DEAP and the layered protocols of TPL and GEO.

[GEO] Geographical Routing + DS-CDMA + Distributed Power Control+ MI Channel Model

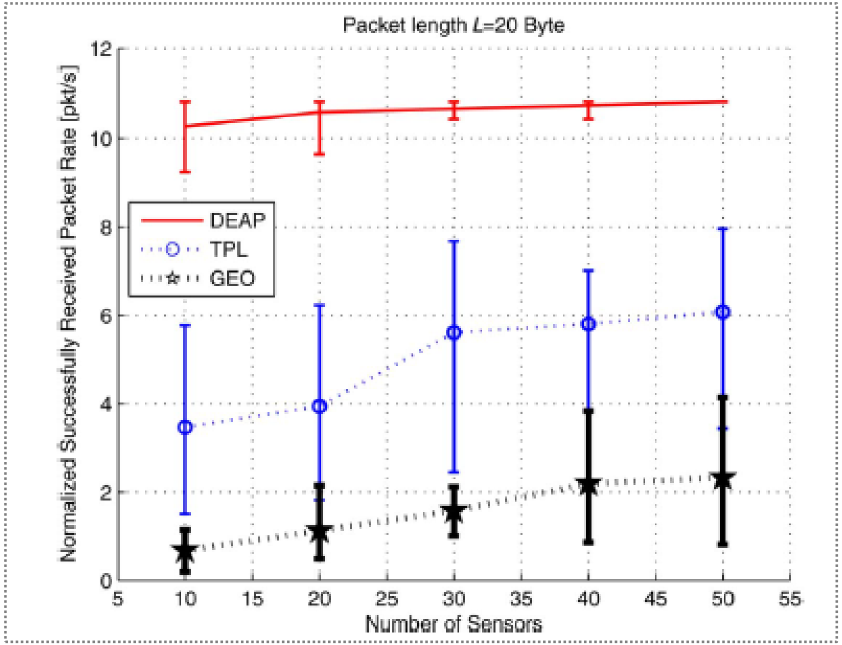

Normalized successfully received packet rate for the cross-layer DEAP and the layered protocols of TPL and GEO.

[GEO] TPL-Based Greedy Routing + DS-CDMA+ Distributed Power Control + MI Channel Model

Highlights: Cross-layer Design

- The interaction of key underground communication functionalities is addressed.
- A distributed cross-layer design, the distributed environment-aware protocol (DEAP), is developed to efficiently utilize the bandwidth-limited MI channels in WUSNs.
- By analytically solving the cross-layer framework with respect to the given code length, statistical delay constraints are guaranteed and the optimal link throughput is achieved.
- A two-phase decision strategy is employed to sequentially tackle two sub-problems for the best feasible energy savings and throughput gain, enjoying low computation complexity for great practicability.
- Performance evaluation confirms that the DEAP provides high throughput and very low energy consumption within a guaranteed delay.

Gen I R&D Milestones

1. Cross-layer Design

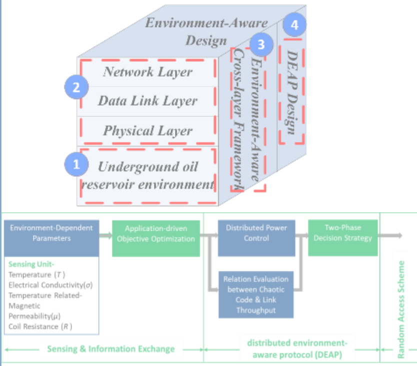

Algorithm 1 Distributed Cross-layer Link Optimization

Input: $i, j, r_{ij}, \theta_{ij}$

$EaT_{min} = \infty$ % Initialization
for $mod = 1 : |\mathcal{M}|$ **do** % Modulation cycle
  for $fec = 1 : |\mathcal{C}|$ **do** % FEC cycle
    Calculate r^j_{min} via tolerable end-to-end PER Φ^{e2e}_T
    $(EaT_{ij}, P, Q, l) \leftarrow$ **Algorithm** 2$(r^j_{min}, NI_j, r_{ij}, \theta_{ij}, m_{ij}(mod), c_{ij}(fec))$
    if $EaT_{ij} < EaT_{min}$ **then**
      $EaT_{min} = EaT_{ij}$
      $(m, c, P, Q, l)^* = (m(mod), c(fec), P, Q, l)$

Patented in US office

2. FractBots Localization

- RMFS measurements
- Localization Framework
- Fast initial positioning
- Fine-grained positioning

3. Optimal Energy Planning

- Power constraints
- Energy Model framework
- FracBot transmission rates
- FracBot network topology

4. FracBots Design & Testbed

- MI-based FracBot node design
- MI-based FracBot network
- Experimental MI-based testbed

FracBot Localization Model

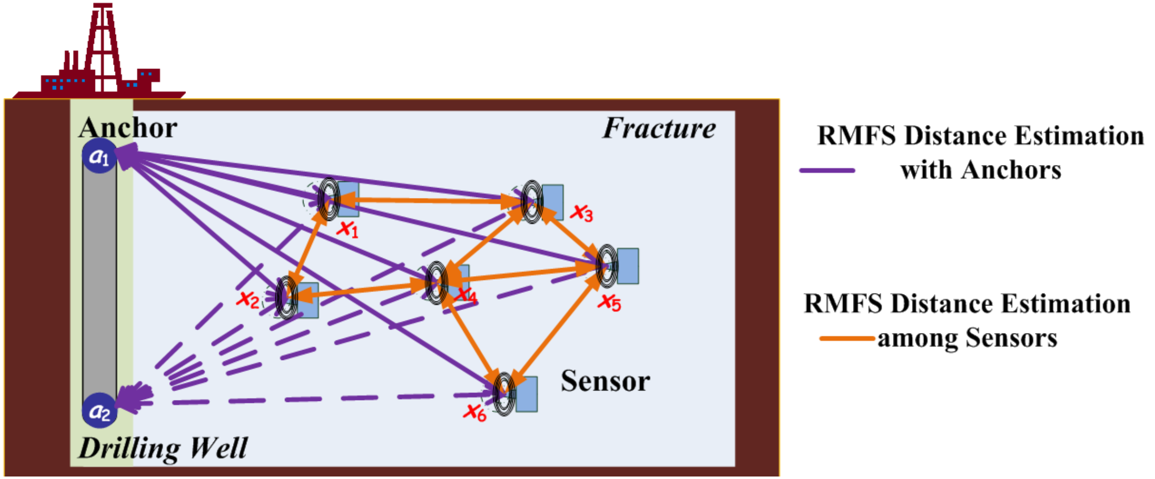

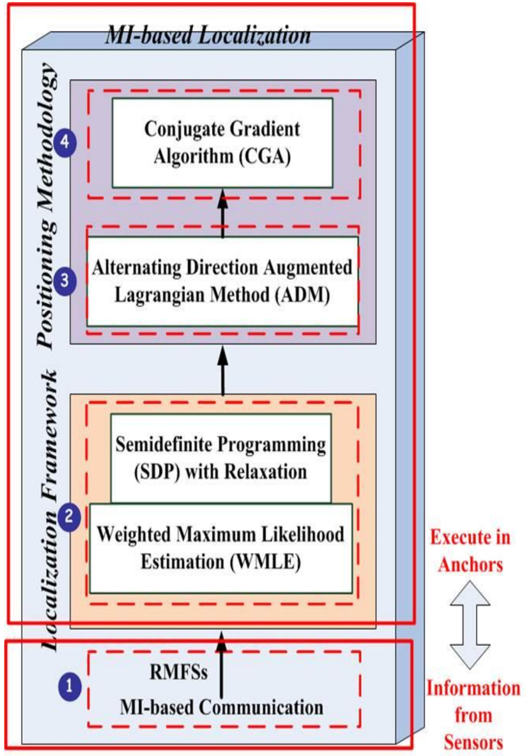

- ➢RMFS (Received Magnetic Field Strength)measurements for designing localization in UOR.
- ➢Localization framework for WUSNs in UOR.
- ➢Fast initial positioning from Alternating Direction Augmented Lagrangian Method (ADM).
- ➢Fine-grained positioning from Conjugate Gradient Algorithm (CGA).

Magnetic Induction-Based Localization

- **Major contributions:**
  - RMFS (Received Magnetic Field Strength) measurements for designing localization in UOR.
  - Localization framework for WUSNs in UOR.
  - Fast initial positioning from Alternating Direction Augmented Lagrangian Method (ADM).
  - Fine-grained positioning from Conjugate Gradient Algorithm (CGA).

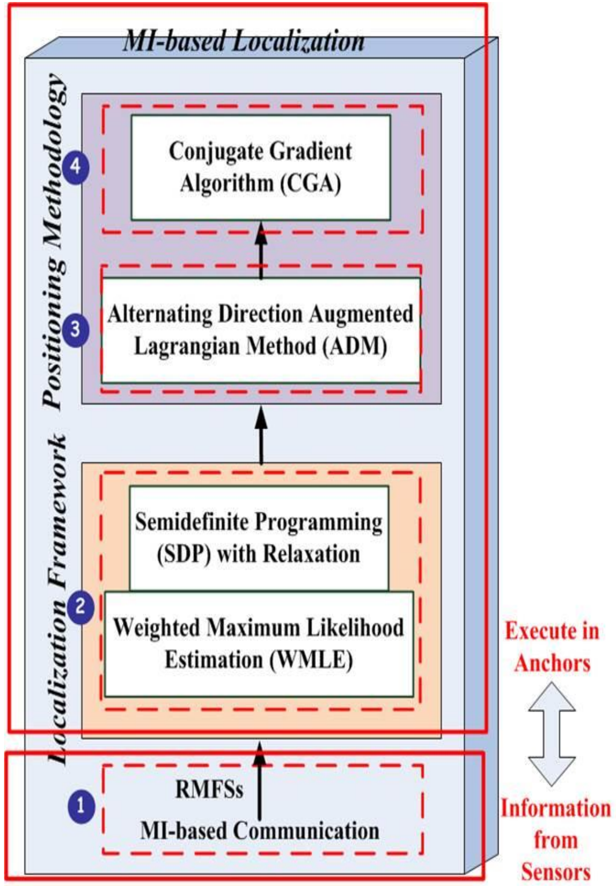

System Model

- ❑ WSNs consists of N sensors with random positions:
  set $\{x_i \in \mathbb{R}^n : 1 \le i \le N\}$
- ❑ Two anchors with known positions:
  set $\{a_k \in \mathbb{R}^n : 1 \le k \le 2\}$.
- ❑ The channel models provide the estimated distances:
  1. among sensors (i.e., d_{ij} , $1 \le i \le N$ and $j \in NH_i$ where NH_i denote the neighbor set of sensor i).
  2. between anchors and sensors (i.e., d_{ik} , $1 \le i \le N$ and $1 \le k \le K$) from the respective RMFS.

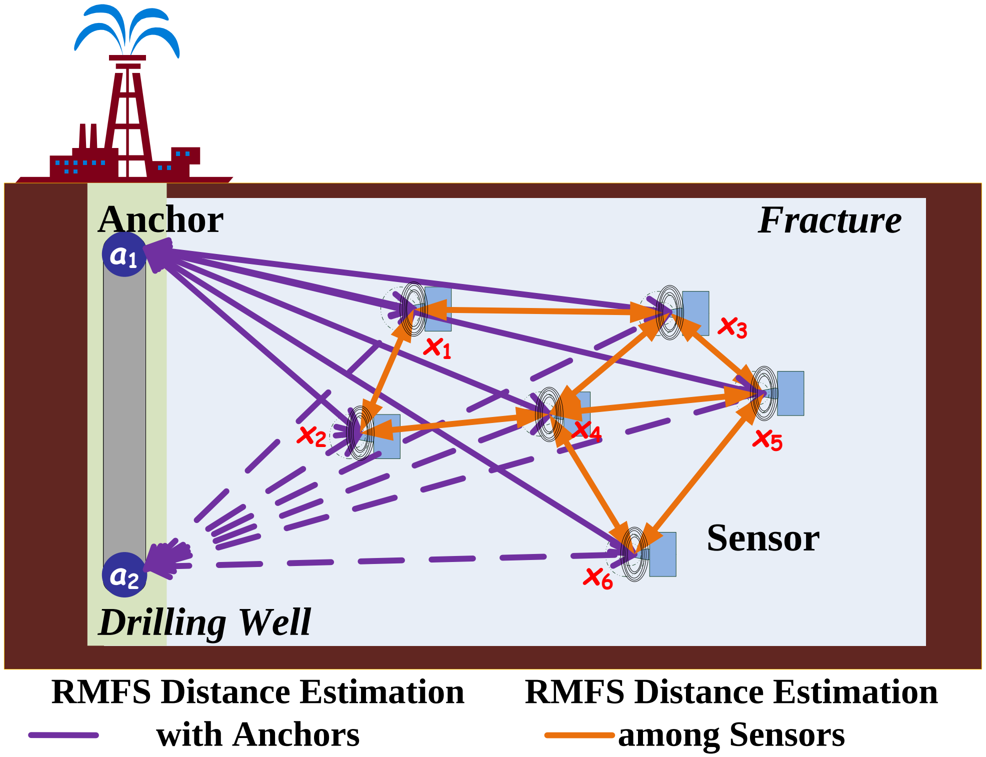

MI-based Localization Framework

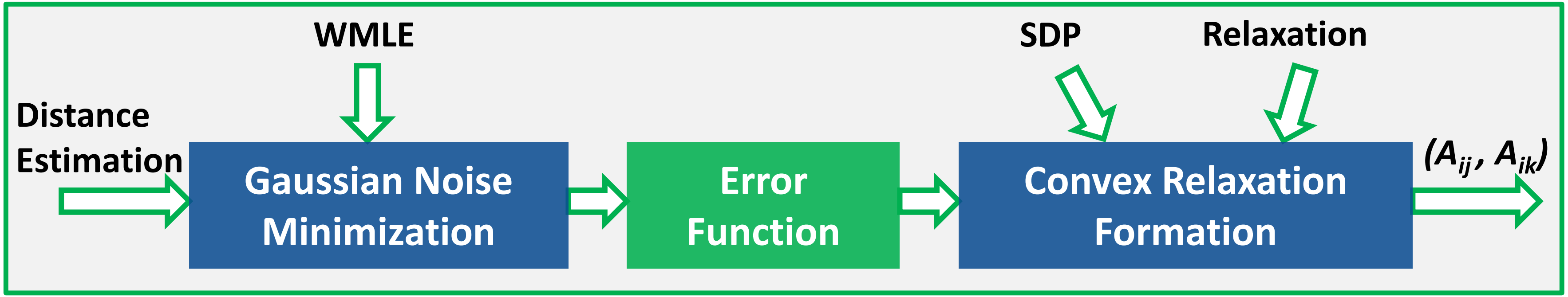

Algorithm 1: ADM-Based Fast-Initial Positioning

Input : $(A_{ij}, \bar{A}_{ik})$, $(\hat{d}_{ij}^2, \hat{d}_{ik}^2)$
$1 \le i \le N, j \in NH_i, 1 \le k \le K$

Output: $x_i, 1 \le i \le N$

Initialize primal $Z^0 \succeq 0$ and dual $\Lambda^0 \succeq 0$
for $m = 0, 1, \ldots$ **do**
  Calculate ϵ^{m+1} from Eq. (14)
  Calculate V^{m+1}, U^{m+1}, eigenvalue decomposition of U^{m+1}, and Z^{m+1} from Eq. (16)
  Calculated Λ^{m+1} from Eq. (17)
end

Algorithm 2: CGA (Fine-Grained Positioning)

Input : $f(\cdot)$ from Eq. (18), $X^{(0)} := [x_1^T, \ldots, x_N^T]^T$ from **Algorithm 1**

Output: X^* % Sensor location

Set $m = 0$; **compute** $d^{(0)} = -\nabla f(X^{(0)})$
while $\nabla f(X^{(m)}) \neq 0$ **do**
  Compute α_m according to Eq. (23)
  Compute $X^{(m+1)}$ according to Eq. (21)
  Compute β_m according to Eq. (23)
  Compute $d^{(m+1)}$ according to Eq. (22)
  Set $m = m + 1$
end
Set $X^* = X^{(m)}$

Performance Evaluation

Fast initial positioning

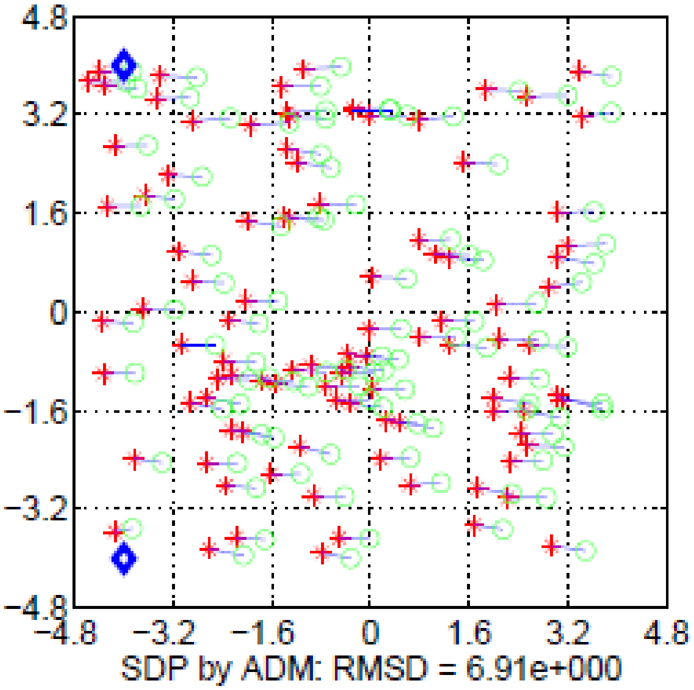

100 sensors with nf=1 after fast initial positioning (ADM).

Fine-grained positioning

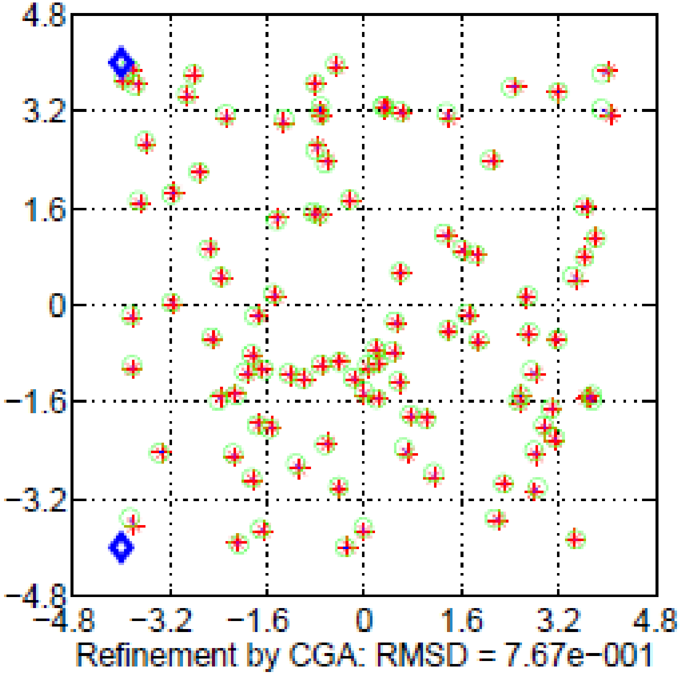

100 sensors with nf=1 after the entire localization (ADM+CGA).

Highlights: Localization

- The fundamental localization challenge in randomly-deployed WUSNs is addressed by exploiting RMFS measurements from MI-based communication
- Proposing fast and accurate successive positioning algorithms.
- Leveraging the multi-path and fading free natures of the MI-based communication, RMFS from AWGN channel modeling serves as the location-dependent information for localization algorithm designs.
- The fast ADM provides useful initial positioning within few iterations
- The powerful CGA refines initial results into highly accurate sensor positions.
- Performance evaluation confirms that the proposed localization guarantees considerable positioning accuracy with great time efficiency in underground environments

Gen I R&D Milestones

1. Cross-layer Design

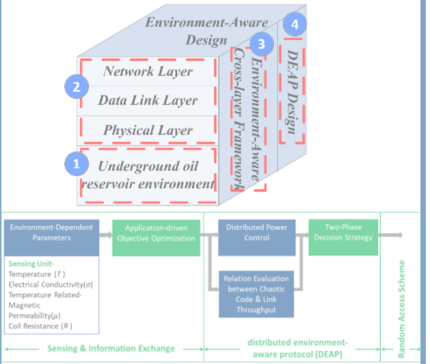

Algorithm 1 Distributed Cross-layer Link Optimization

Input: $i, j, r_{ij}, \theta_{ij}$

1: $EaT_{min} = \infty$ % Initialization
2: **for** $mod = 1 : |\mathcal{M}|$ **do** % Modulation cycle
3: **for** $fec = 1 : |\mathcal{C}|$ **do** % FEC cycle
4: **Calculate** r^j_{min} via tolerable end-to-end PER Φ^{e2e}_T
5: $(EaT_{ij}, P, Q, l) \leftarrow$ **Algorithm** 2$(r^j_{min}, NI_j, r_{ij}, \theta_{ij},$
6: $m_{ij}(mod), c_{ij}(fec))$
7: **if** $EaT_{ij} < EaT_{min}$ **then**
8: $EaT_{min} = EaT_{ij}$
9: $(m, c, P, Q, l)^* = (m(mod), c(fec), P, Q, l)$

Patented in US office

2. FractBots Localization

Algorithm 2 CGA (Fine-Grained Positioning)

Input: $f(\cdot)$, $X^{(0)} := [x_1^T, \ldots, x_N^T]^T$ from **Algorithm 1**
Output: X^* % Sensor location **Set** $m = 0$; **compute** $d^{(0)} = -\nabla f(X^{(0)})$
while $\nabla f(X^{(m)}) \neq 0$ **do Compute** α_m
Compute $X^{(m+1)}$
Compute β_m
Compute $d^{(m+1)}$
Set $m = m + 1$
end whileSet $X^* = X^{(m)}$

Patented in US office

3. Optimal Energy Planning

- Power constraints
- Energy Model framework
- FracBot transmission rates
- FracBot network topology

4. FracBots Design & Testbed

- MI-based FracBot node design
- MI-based FracBot network
- Experimental MI-based testbed

Optimal Energy Planning & Management

Three-stage operational structure

1. **An one-hop radiative energy charging stage**
   - Downlink: A large dipole antenna radiates RF signals to charge sensors via direct transmissions
   - Steady power source for sensors
   - Depend on the distance (Sn has the best charging efficiency)
2. **A multi-hop MI-communications stage**
   - Uplink: Sensors transmit sensing data to the drilling well (station) through hop-by-hop MI transmissions
   - Joint design of unique MI channel characteristic with communication functionalities
3. **A backbone communications stage**

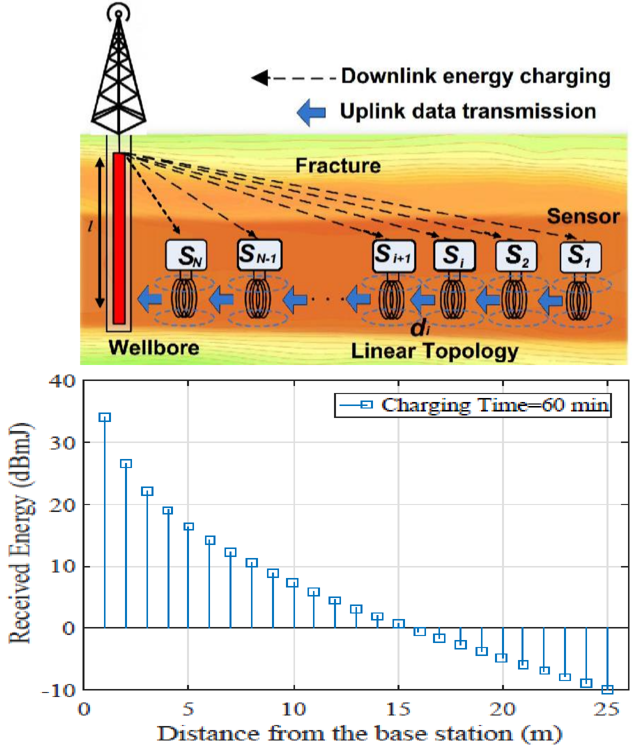

Coherent Energy Charging & Consumption

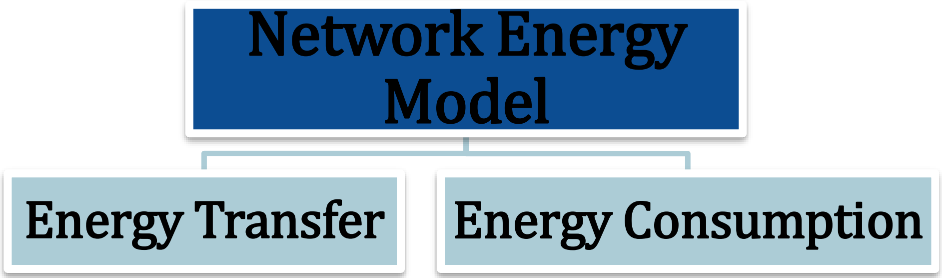

Energy constraint:

$$E^{\text{received}} \geq E^{\text{consumed}}$$

E^{received}: harvested energy by sensor nodes from Base Station

E^{consumed} : consumed energy by sensors due to
(1) sensing; (2) processing; (3) communication

Optimal Energy Planning & Management

Optimal energy planning — Reformulate → **Simplified optimal energy planning**

$$\max_{\{\lambda_i\},N} \sum_{i=1}^{N} \lambda_i$$
$$\text{s.t.} \quad 1-(1-\Phi_i(d_i))^i \le \Phi_T^{e2e}, \ \forall i \in N;$$
$$\sum_{j=1}^{i} \lambda_j R_j^C (E_b^{MI}(d_j) + 2E_b^{elec}) \le E_i^h, \ \forall i \in N$$

$$\max_{\lambda,N} N\lambda$$
$$\text{s.t.} \quad 1-(1-\Phi(d))^N \le \Phi_T^{e2e};$$
$$i\lambda R^C (E_b^{MI}(d) + 2E_b^{elec}) \le E_i^h, \ \forall i \in N$$

Algorithm Fast Optimal Energy Planning.

- **set** $N = 1$
- **repeat**
  - **calculate** $\lambda^N = \min_{i \le N} E_i^h / [iR^C(E_b^{MI}(d) + 2E_b^{elec})]$
  - **set** $N := N + 1$
- **until** $N > \log_{(1-\Phi(d))}(1-\Phi_T^{e2e})$
- $N^* = \arg\max_i i\lambda^i$ **and** $\lambda^* = \lambda^{N^*}$ =0

Performance Evaluation

Received energy

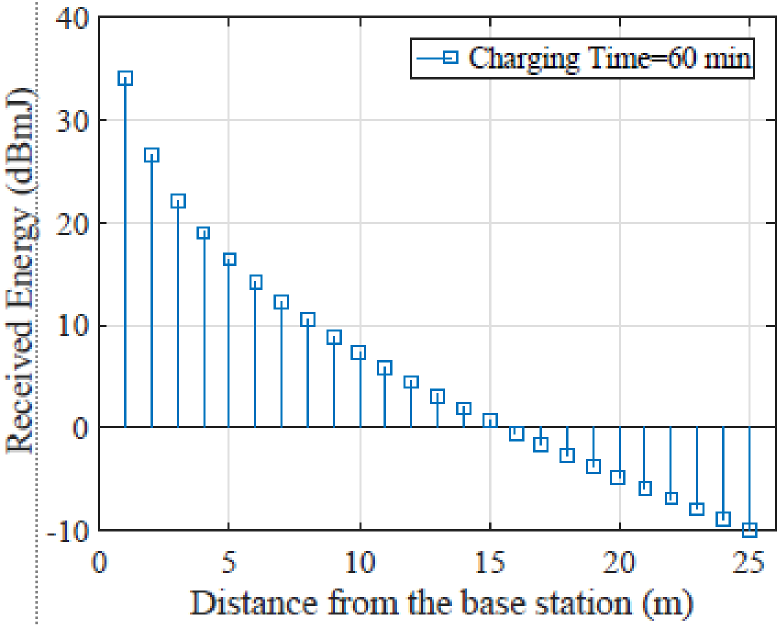

Energy received by sensors from the base station

Optimal transmission rate

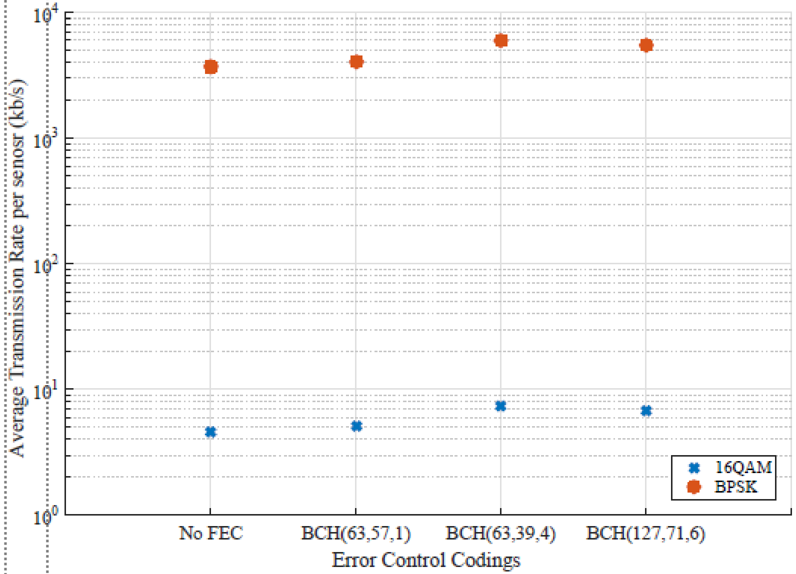

Optimal transmission rate for BPSK and 16QAM modulation techniques and BCH(n,k,t) coding schemes.

Gen I R&D Milestones

1. Cross-layer Design

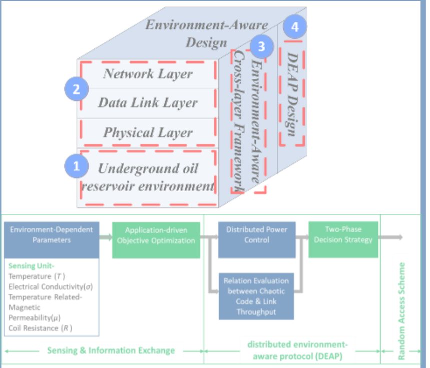

Algorithm 1 Distributed Cross-layer Link Optimization

Input: $i, j, r_{ij}, \theta_{ij}$

1: $EaT_{min} = \infty$ % Initialization
2: **for** $mod = 1 : |\mathcal{M}|$ **do** % Modulation cycle
3: **for** $fec = 1 : |\mathcal{C}|$ **do** % FEC cycle
4: **Calculate** r^j_{min} via tolerable end-to-end PER Φ^{e2e}_T
5: (EaT_{ij}, P, Q, l) ←**Algorithm 2**$(r^j_{min}, NI_j, r_{ij}, \theta_{ij}, m_{ij}(mod), c_{ij}(fec))$
7: **if** $EaT_{ij} < EaT_{min}$ **then**
8: $EaT_{min} = EaT_{ij}$
9: $(m, c, P, Q, l)^* = (m(mod), c(fec), P, Q, l)$

Patented in US office

2. FractBots Localization

Algorithm 2 CGA (Fine-Grained Positioning)

Input: $f(\cdot)$, $X^{(0)} := [x_1^T, \ldots, x_N^T]^T$ from **Algorithm 1**

Output: X^* % Sensor location **Set** $m = 0$; **compute** $d^{(0)} = -\nabla f(X^{(0)})$

while $\nabla f(X^{(m)}) \neq 0$ **do Compute** α_m
Compute $X^{(m+1)}$
Compute β_m
Compute $d^{(m+1)}$
Set $m = m + 1$
end whileSet $X^* = X^{(m)}$

Patented in US office

3. Optimal Energy Planning

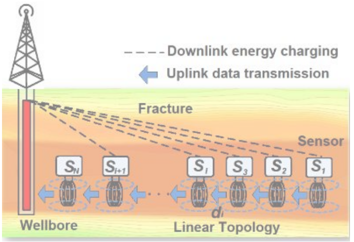

Algorithm 1 Fast Optimal Energy Planning.

set $N = 1$
repeat
calculate
$\lambda^N = \min_{i \leq N} E_i^h / [iR^C(E_b^{MI}(d) + 2E_b^{elec})]$
set $N := N + 1$
until $N > \log_{(1-\Phi(d))}(1 - \Phi_T^{e2e})$
$N^* = \arg\max_i i\lambda^i$ and $\lambda^* = \lambda^{N^*}$

Published in IEEE ICC Conference

4. FracBots Design & Testbed

- MI-based FracBot node design
- MI-based FracBot network
- Experimental MI-based testbed

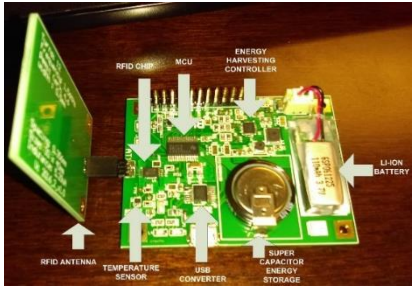

FracBot Node Design Roadmap

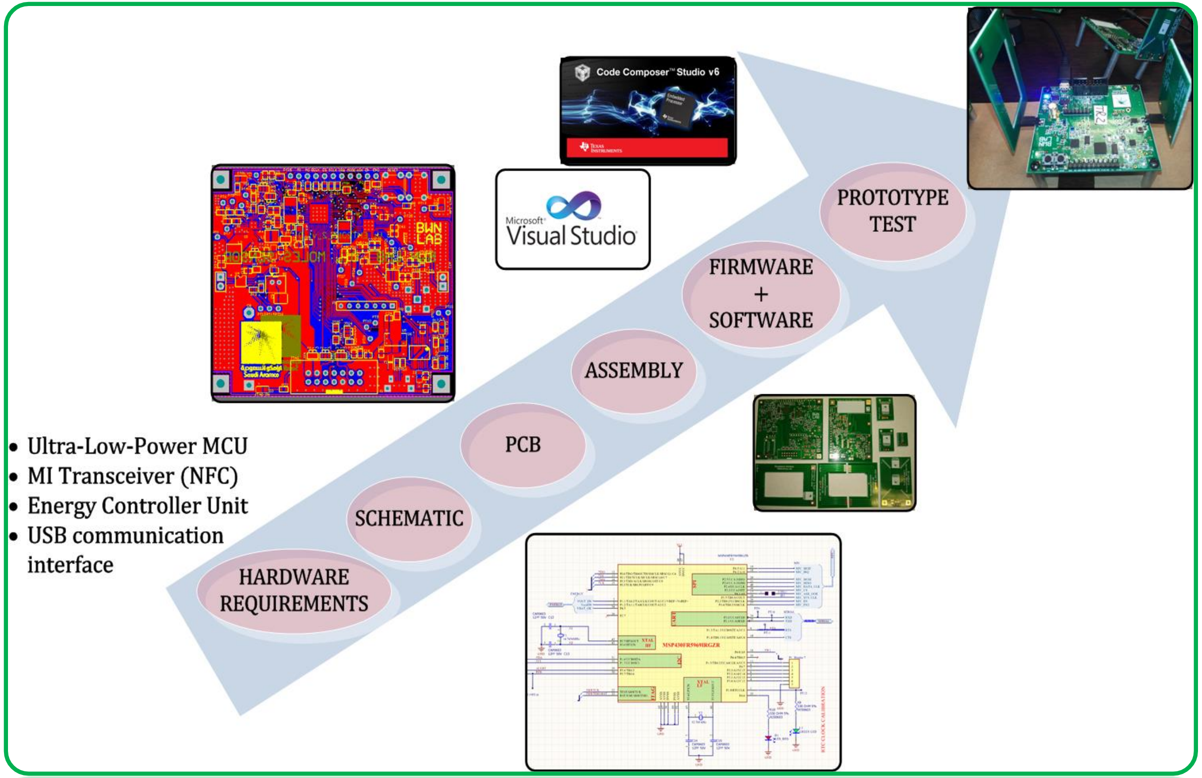

- Ultra-Low-Power MCU
- MI Transceiver (NFC)
- Energy Controller Unit
- USB communication interface

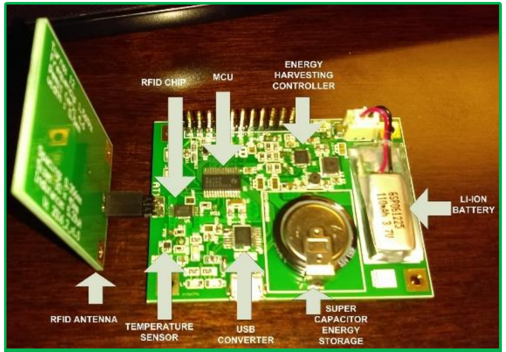

- Prototype of Frac

FracBot Design Requirements

- Long operation time through ultra-low-power electronics
- Advanced low-power microcontroller
- Efficient underground communication layer
- Energy-harvesting capability
- Sensing capability

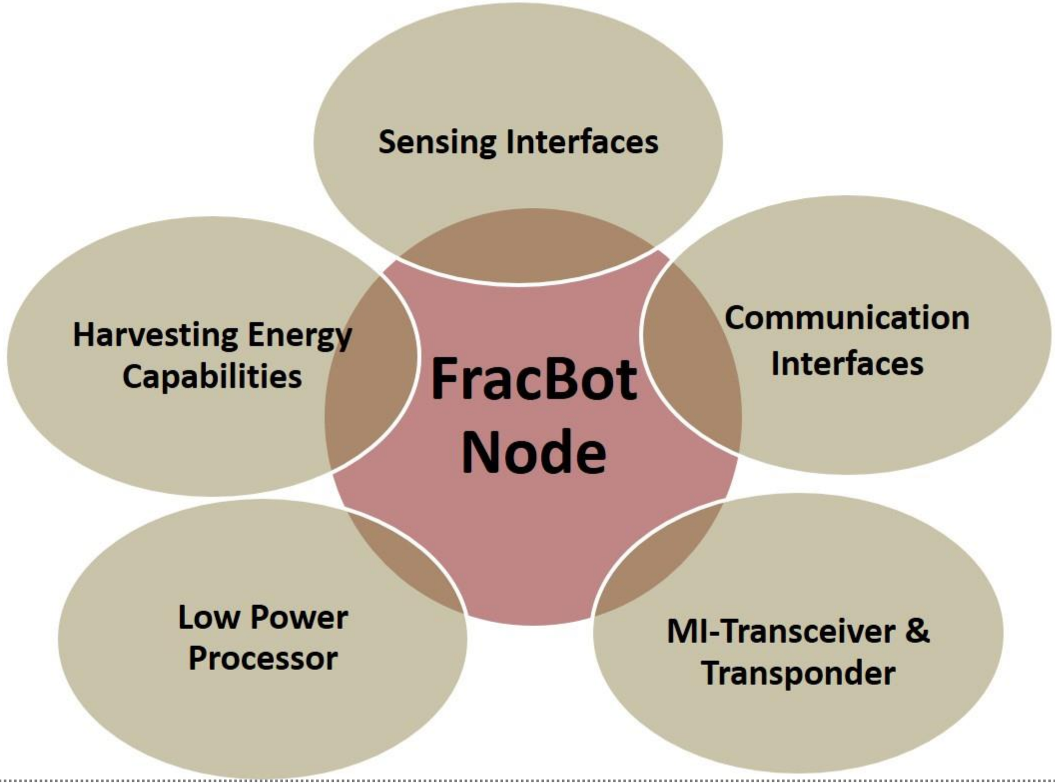

Implementation Process

- **Components selection**
- Applications compatibility
  - Out-of-shelf components
- **Schematic drawing**
  - Shows components and the interconnections.
- **PCB design**
  - create the physical interconnections (routes) to start the board production
- **Components assembly**
  - components are soldered to the PCB in their positions.
- **Firmware and software coding**
  - A code operates the FracBots & software to manages the system.
- **Testing and verification**

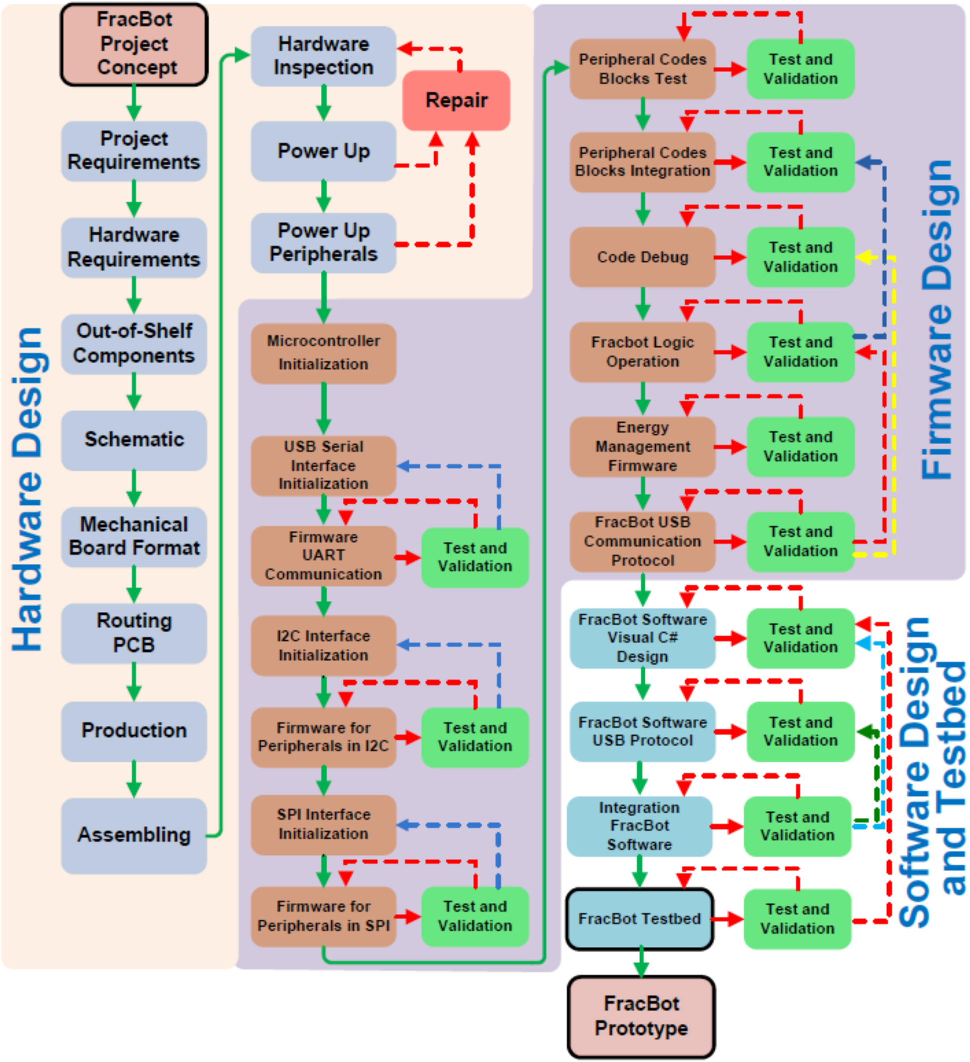

FracBot Hardware Design

- **A compact MI coil antenna**
  - Big traditional antennas is not applicable in oil reservoir environnent
- **The MI field**
  - can penetrate a high-loss oil reservoir media
- **Launch constant MI channel**
  - Enables wireless MI communication
- **Energy harvesting**
  - inside the hydraulic fracture and oil reservoir environment

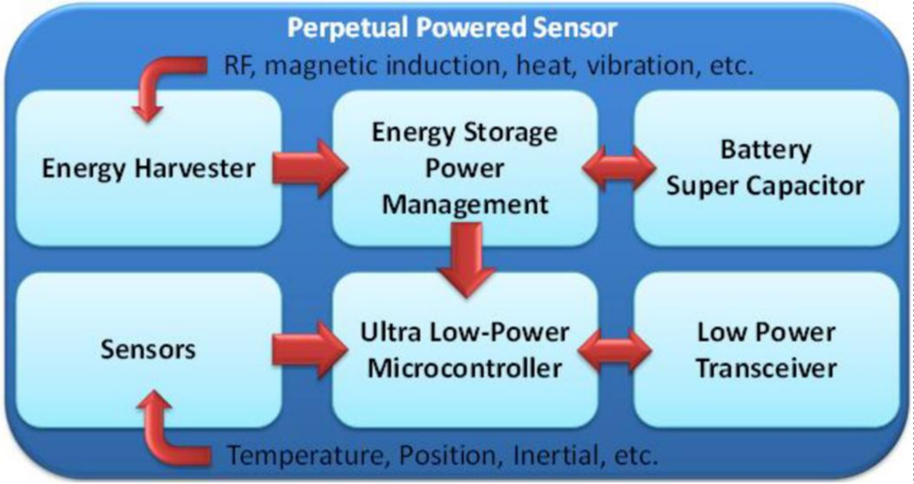

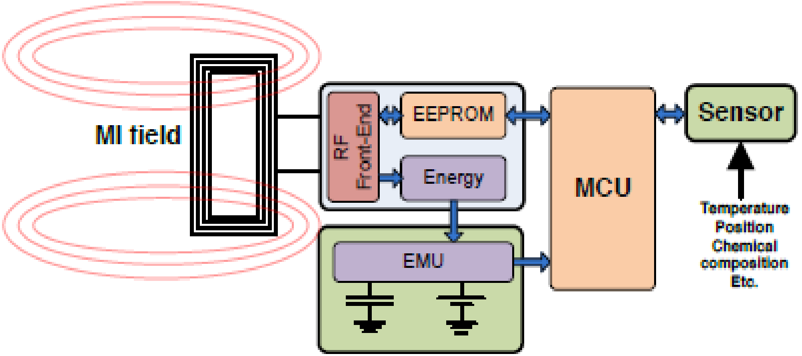

FracBot Gen I Prototype

- FracBot: a proof of concept
- Characteristics
  - PCB planar coil (two layers)
  - NFC tag with EEPROM Memory and energy harvesting
  - Receiver antenna
  - Energy management unit (EMU)
  - Ultra-low power microcontroller
  - Ultra-low power temperature sensor
  - Supercapacitor or Rechargeable battery
  - USB interface (debug and Laboratorial test)
  - NFC transceiver chip
  - NFC transceiver antenna

FracBot Active Node

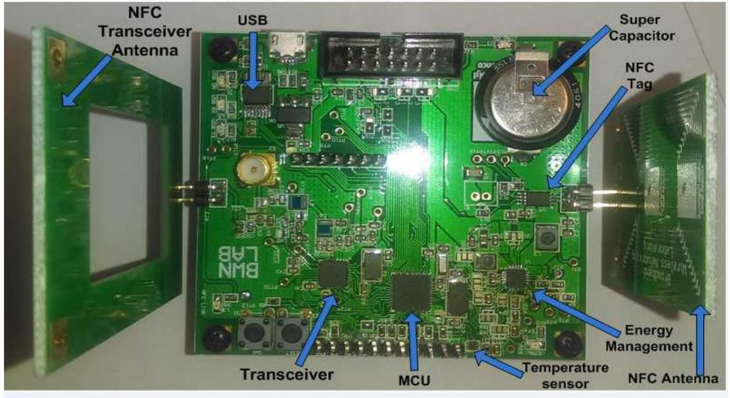

FracBot Passive Node

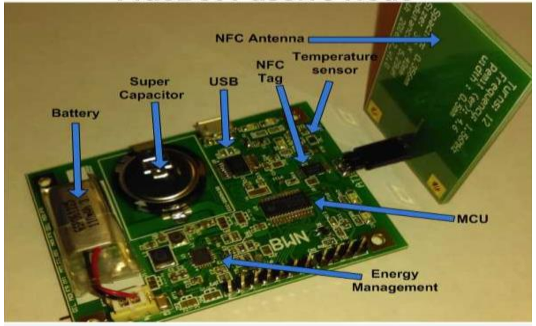

Energy-Harvesting Management Unit

- Main components of energy harvesting process :
    1. NFC transponder
    2. Energy management unit (Nanopower Harvesting Energy Controller)
- Energy Harvested from the exceeded energy of NFC field.
- Power control through Maximum Power Point Tracking (MPPT).
- Regulated voltage output and signal indication of available energy.

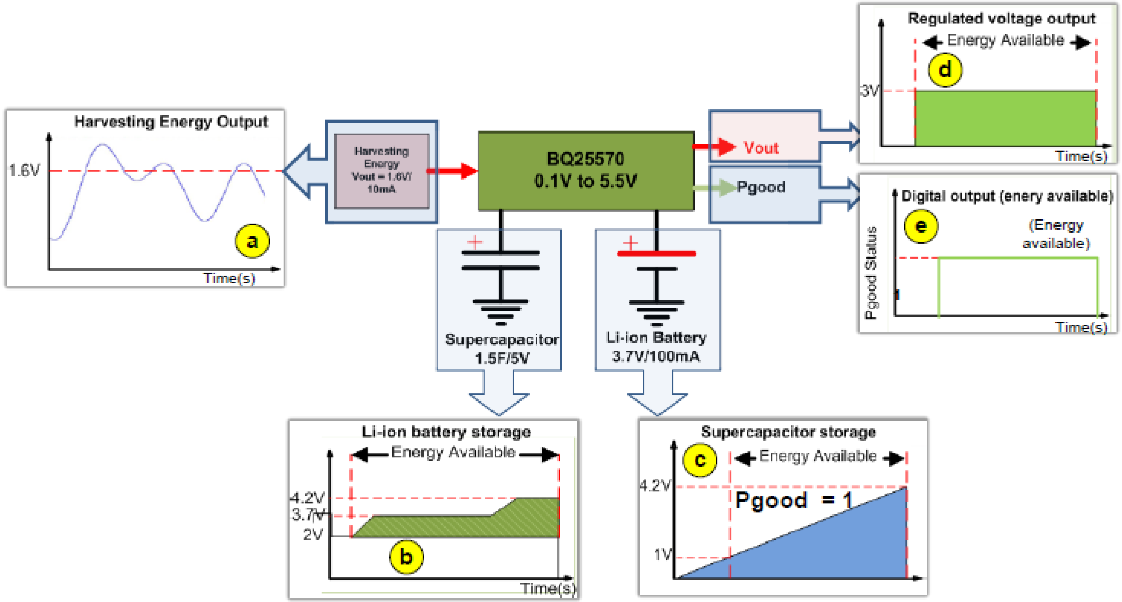

Voltage Ranges for All Components

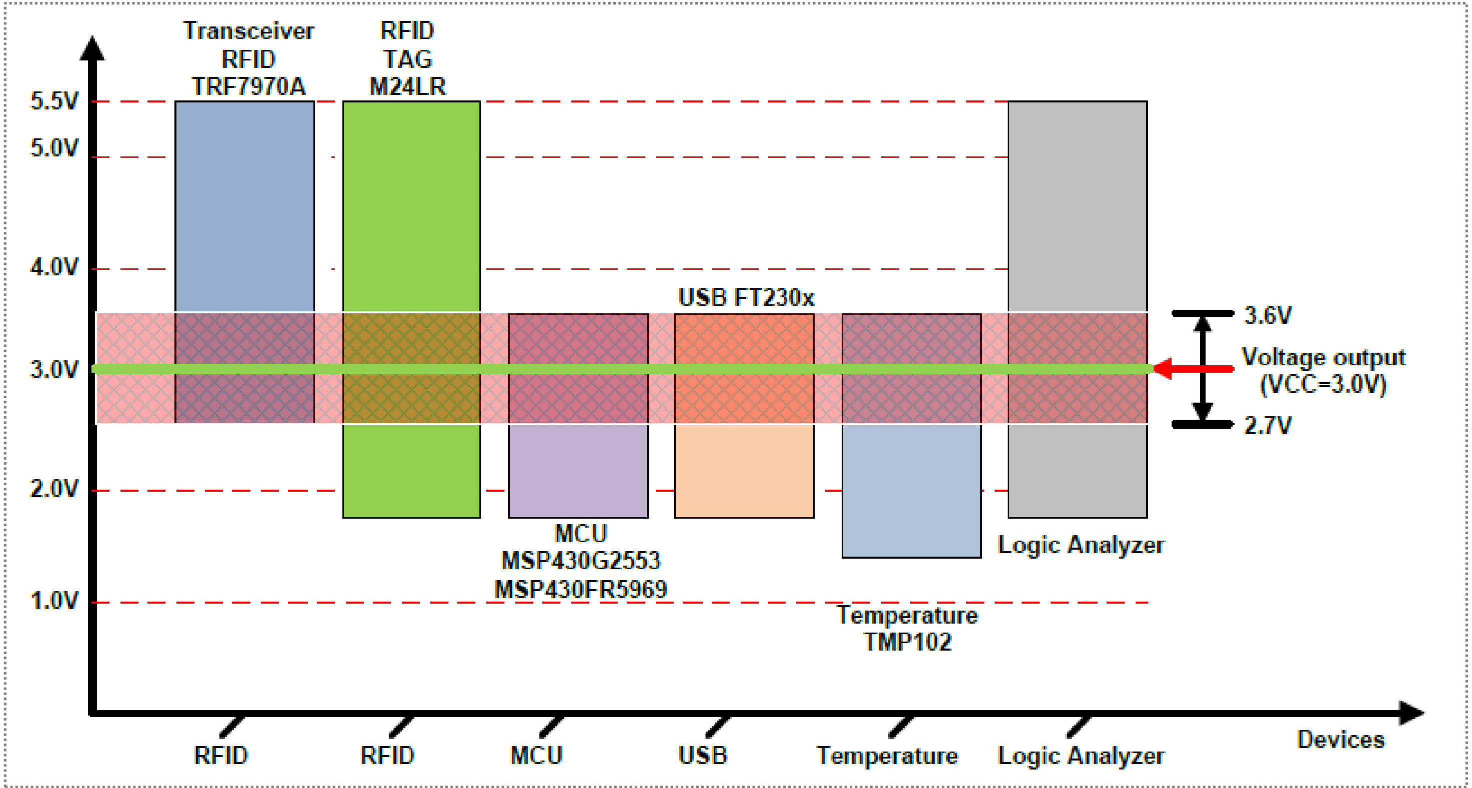

The controller EMU BQ25570 is configured to generate **3 volts**

Energy Measurement and Management

- Measuring the current and power in ultra low energy circuits is the main step to reach an optimal design and an efficient power management.
- The shunt resistor or sensing resistor are reliable and precise techniques
- The measurement system used in the FracBot energy analysis is based on chip PAC1934 (Microchip)

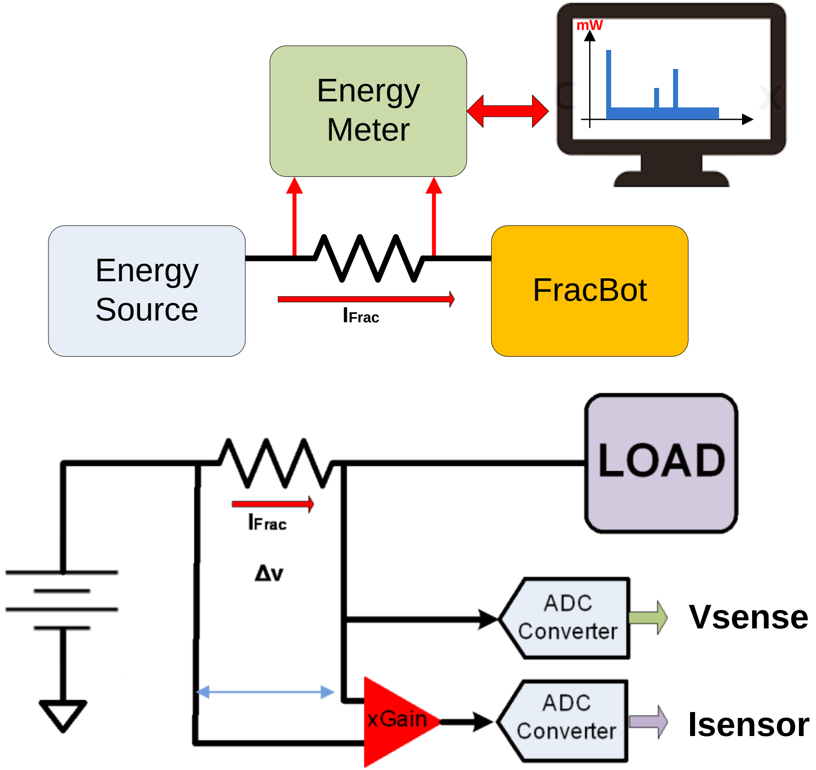

FracBot Energy Consumption Circuit

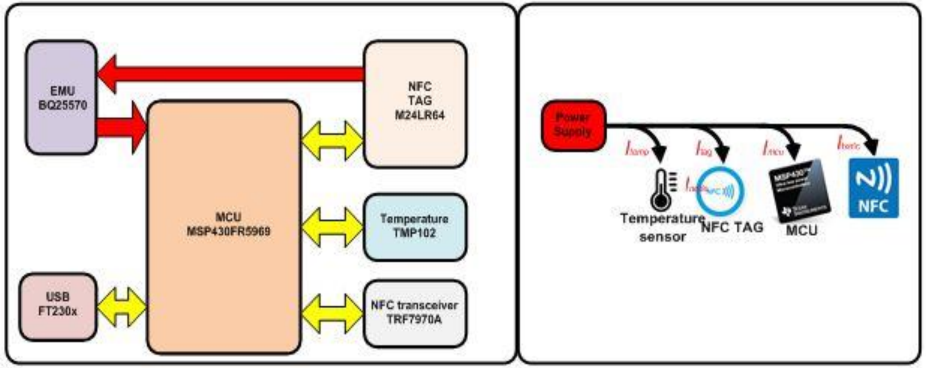

Active Node: Energy Consumption Circuit

Function	Active Mode	LPM mode	Sleep Mode
Temperature Sensor	10 µA	n/a	1µA
Microcontroller	100 µA/MHz @ 2.2V	0.9 µA @ 2.2V	0.02µA @ 2.2V
Transceiver NFC	78 mA@20dBm (100mW)	120 µA	1 µA
Passive NFC tag	100 µA	n/a	30 µA

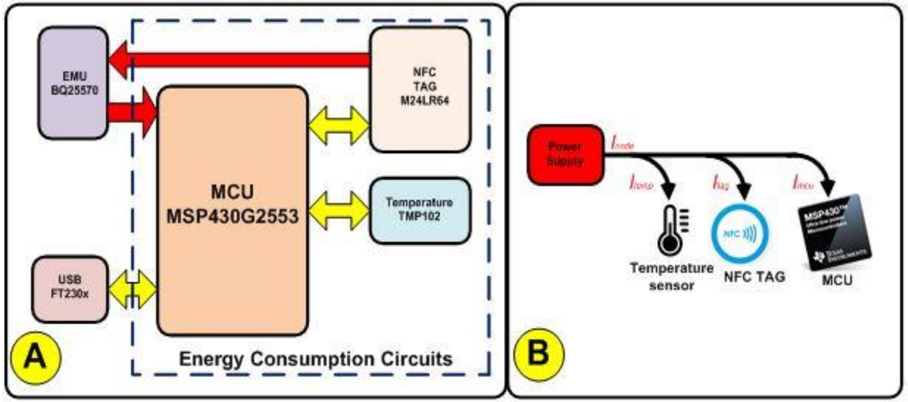

Passive Node: Energy Consumption Circuit

Function	Active Mode	LPM 2 mode	Sleep Mode
Temperature Sensor	10 µA	n/a	1 µA
Microcontroller	230 µA/MHz @ 2.2V	22 µA@ 2.2V	0.1µA@ 2.2V
Passive NFC tag	100 µA	n/a	30 µA

FracBot Energy Measurement Testbed

- The power analyzer testbed
- Necessary to calculate the optimized shunt resistor to improve the reading
- The testbed consists of
  - An adjustable shunt/ sensor resistor
  - A power meter chip PAC1934
- The energy estimation in the passive and active FracBots were realized in two main steps:
  - Individual power peripheral measurement
  - The entire sensor node power measurement

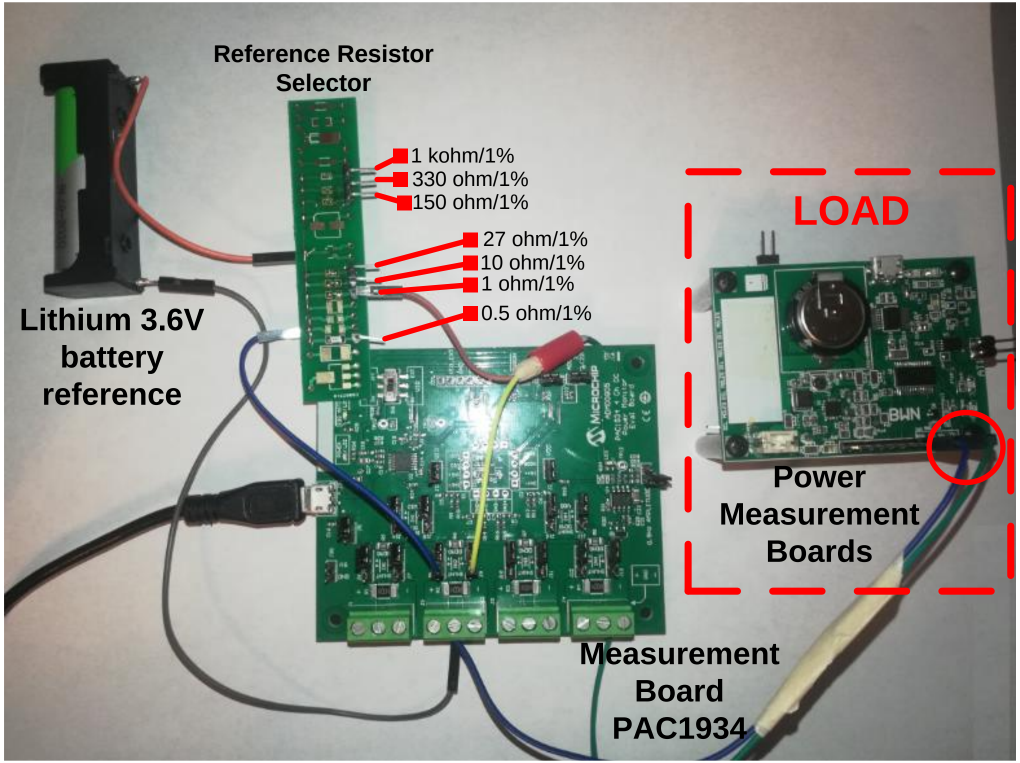

FracBot Passive node Energy Analysis

- The power measurement was realized through the sectioned circuits
- The power lines in the PCB board were cut to segregate individual circuits
- The node executes 1 reading/ hour in ultra low power mode, the estimated energy is **173µW/h**
- During the full shutdown of the system, the power is $103\mu W/h$

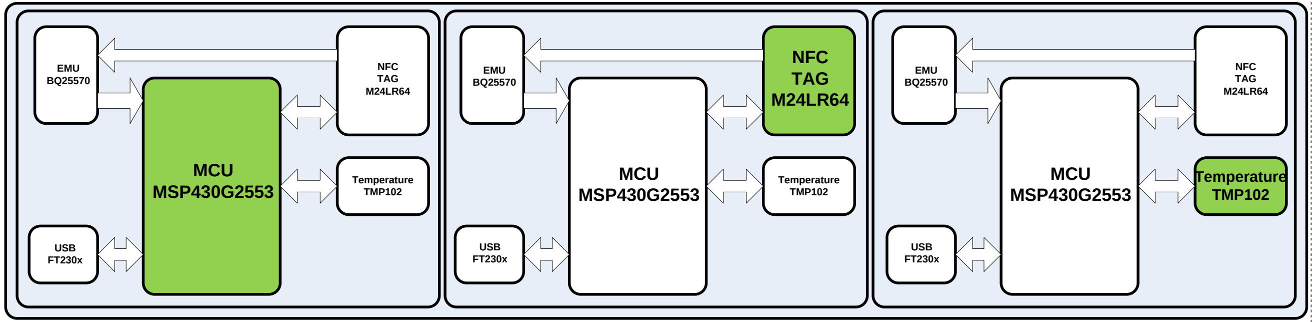

Peripheral	Theoretical Current (µA)	Measured Current (µA)	Reference Resistor	Energy (mWh) Measured
MCU (Active Mode) (MSP430G2553)	230 µA@2.2V	252 µA@3.4V@1MHz	330 Ω	850 µWh
MCU (LPM) (MSP430G2553)	22 µA/@2.2V	31µA@3.4V	1 kΩ	102 µWh
NFC Tag (M24LR64)	100 µA (Active) 30 µA (LPM)	98 µA (Active) 31 µA (LPM)	330 Ω	333 µWh (Active) 102 µWh (LPM)
Temperature Sensor (TMP102)	10 µA(Active) 1 µA (LPM)	12 µA (Active) 1.3 µA (LPM)	1k Ω	333 µWh (Active) 102 µWh (LPM)
FracBot Node	362 µA (Active) 53 µA (LPM)	398 µA (Active) 79 µA (LPM)	330 Ω	1.37 mWh (Active) 278 µWh (LPM)

FracBot Passive node Energy Analysis

- The firmware of the FracBot passive node for this measurement has data format conversions instruction to write in decimal format and store in the NFC tag.
- The energy consumption decreases over 70% using the code optimization and the hexadecimal data storage.

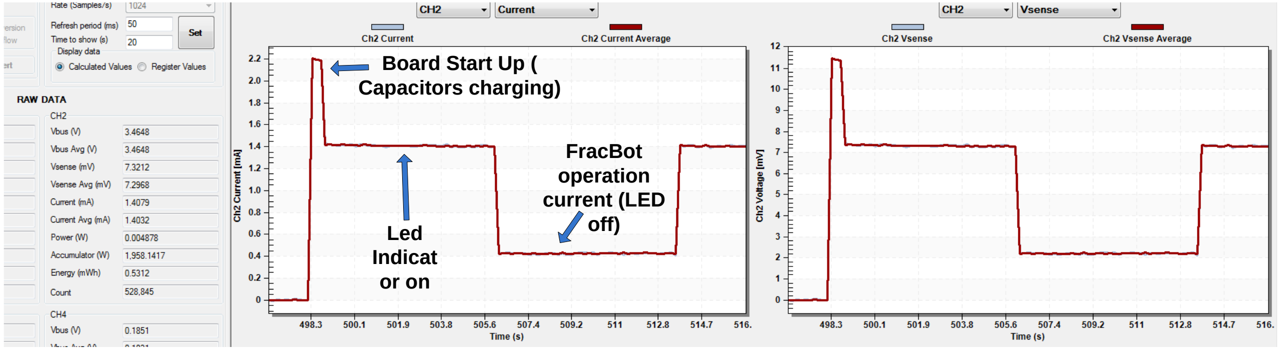

Logic analyzer – communication time estimation

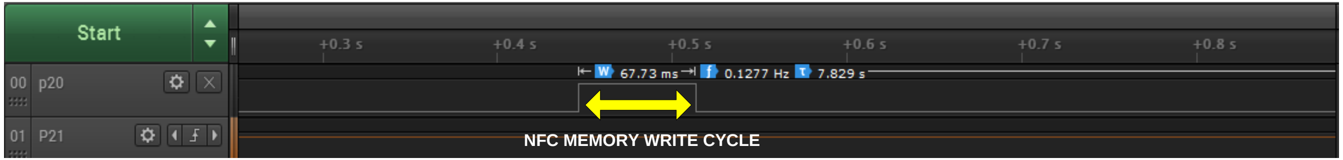

FracBot Active Node Energy Analysis

- The NFC transceiver consumes over 70 times of the power consumed by the microcontroller.
- The measured current of the microcontroller is 1.8 mA while the one of the NFC transceiver is 114 mA.
- The node executes 1 reading/ hour in ultra-low power mode, the estimated energy is **24. 7mW/h**
- During the full shutdown of the system after the reading and memory transfer, the power is **24.69 mW/h**

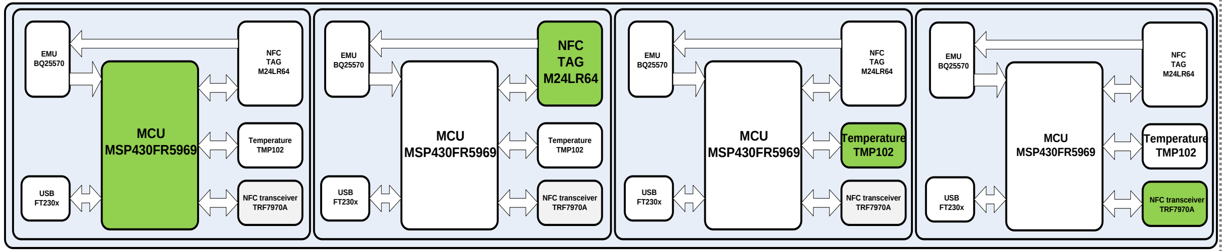

Peripheral	Theoretical Current/Power	Measured Current	Reference Resistor	Energy (mWh)
MCU (Active Mode) (MSP430FR5969)	100 µA/MHz	1.8 mA@16MHz	330 Ω	6.12 mWh
MCU (LPM) (MSP430FR5969)	0.9 µA	1.2 µA	1 kΩ	41 µWh
NFC Tag (M24LR64)	100 µA (Active) 30 µA (Active)	102 µA (Active) 28 µA (LPM)	330 Ω	346 µWh (Active) 95 µWh (LPM)
Temperature Sensor (TMP102)	10 µA(Active) 1 µA (Active)	11 µA (Active) 1.1 µA (LPM)	1 kΩ	37 µWh (Active) 3.7 µWh (LPM)
NFC transceiver (TRF7970A)	130 mA (Active 20 dbm)	112 mA (Active 20 dbm)	1 Ω	381 mWh (Active)
FracBot Node	130 mA	118 mA	1 Ω	401 mWh (Active)

FracBot Active Node Energy Analysis

- The microcontroller power consumptions represents 0.01% only for the energy in active mode.
- The difference is due to the microcontroller technology used in this design, the technology FRAM provides very low energy consumption.
- The data transmission using hex code enable a compact data stream and reduce the communication time.
- The transceiver is responsible for 99.9% of the required energy.
- Optimizing data storage and data transmission techniques can provide energy reduction over 20%.

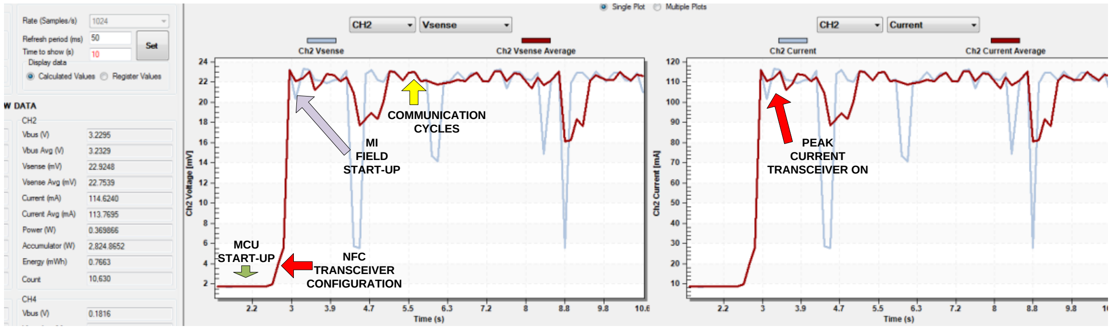

Logic Analyzer

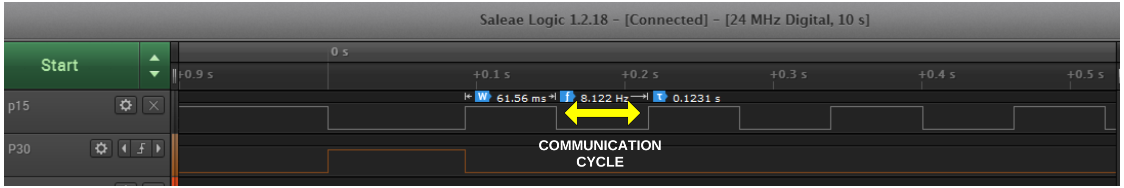

The FracBot Testbed

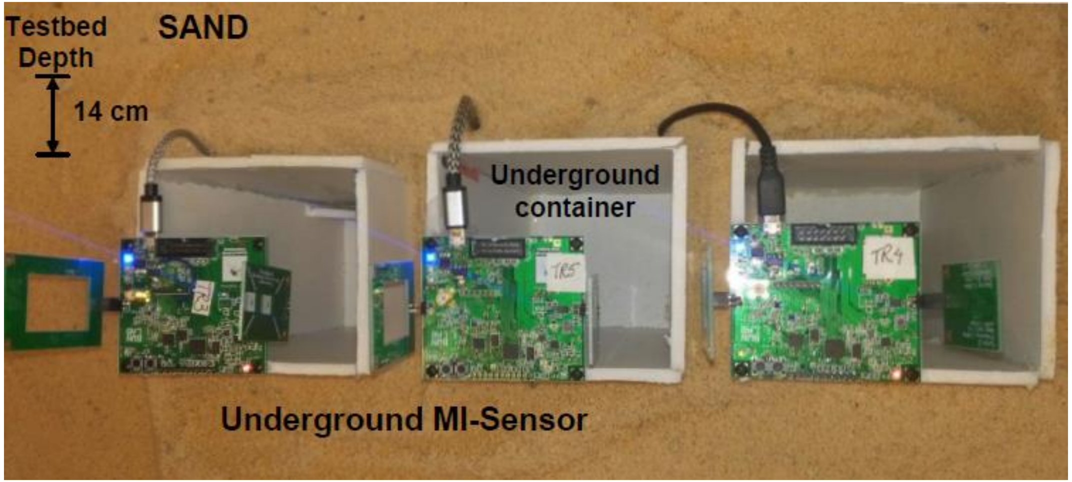

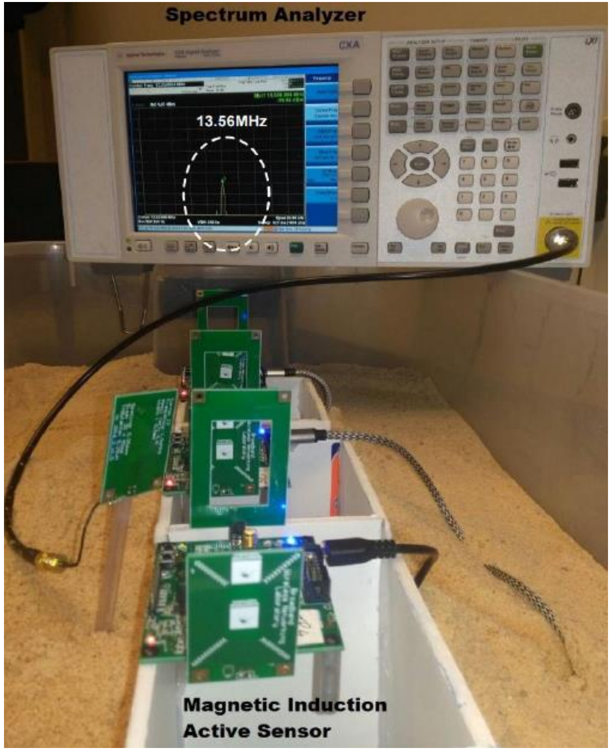

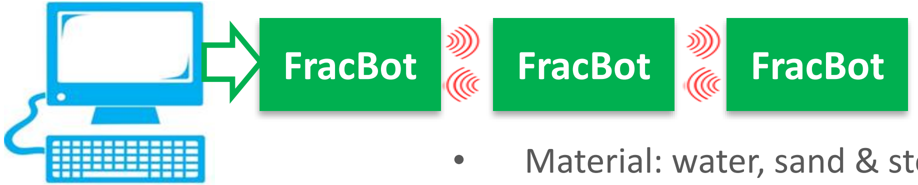

Testbed characteristics:

- Material: water, sand & stone.
- Depth: 14 cm
- Operational distance: 5 cm

Experimental Performance of Communication Link

- Comparative results based on standard communication data rate provided by the NFC chips
- Environment: air, sand & stone (underground testbed)
- The low data rate is consequence of the high path loss posed by underground environment

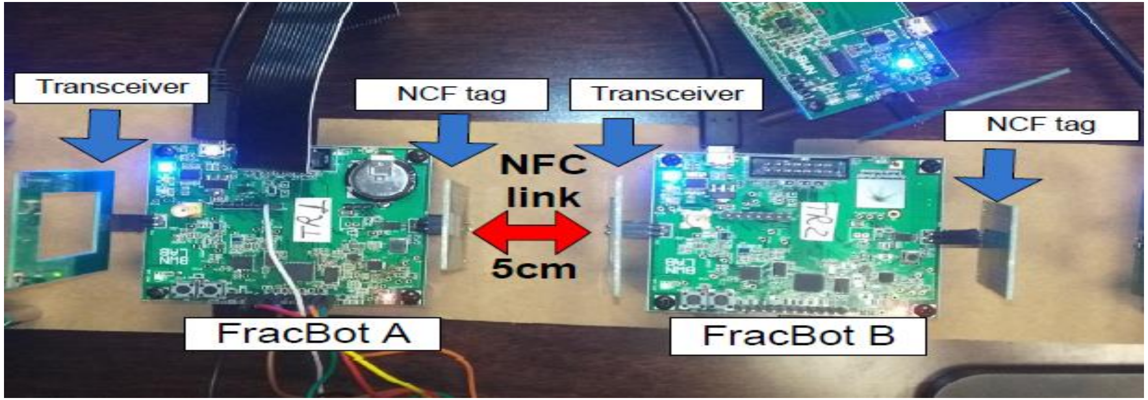

Environment	Modulation	Data rate (kbit/s)	Error (%)
Air	ASK	26	2
Air	OOK	26	1

FracBot Experimental Setup

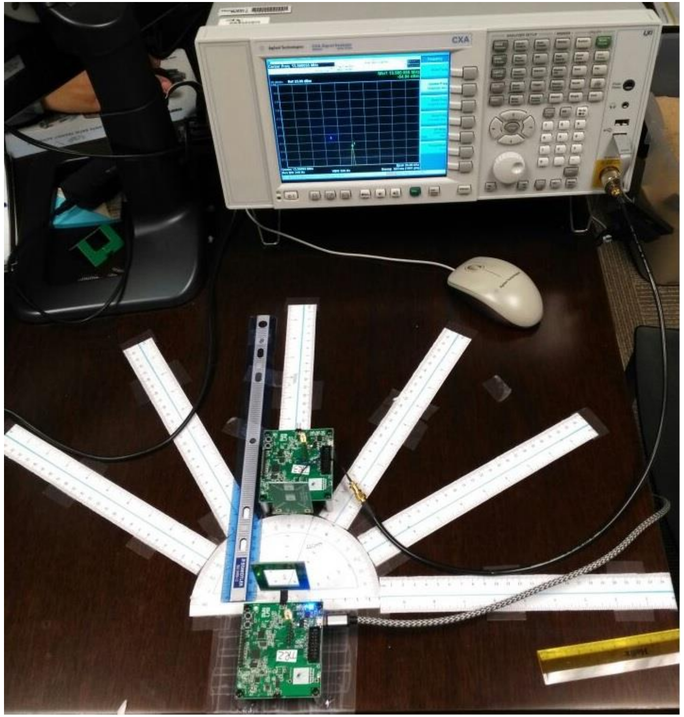

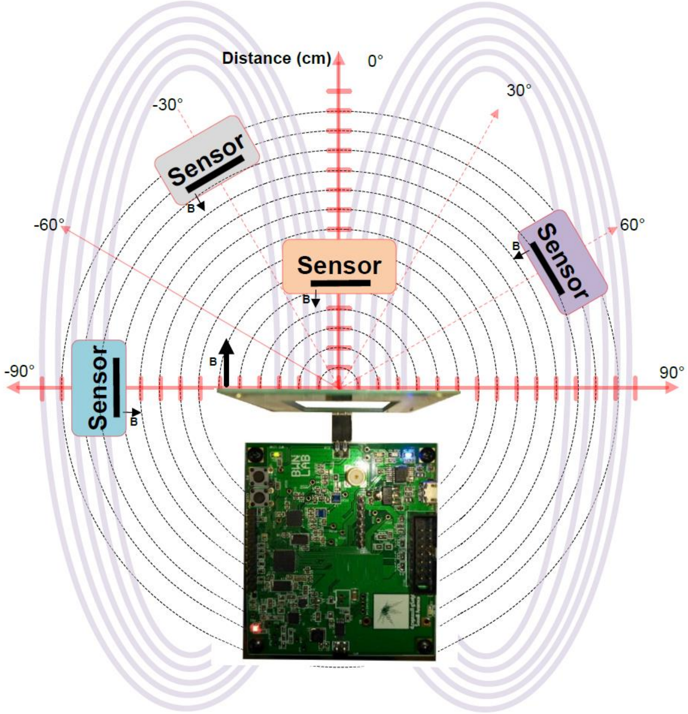

- The MI interaction is measured in distances between 0 and 25cm and angles of 0, 30, 60 and 90 degree, respectively.

Angular Analysis

- **One of the problems in MI-based communication is the orientation and alignment between the transceiver and receiver of the FracBots.**

- For distances beyond **6 cm**, the angle between the transceiver and the receiver antenna does not affect the received power that much, only lower **than 2 dBm**.

- Intense power can be received occurs beyond 6cm in air at signal strength between **-45 and -55** dBm.

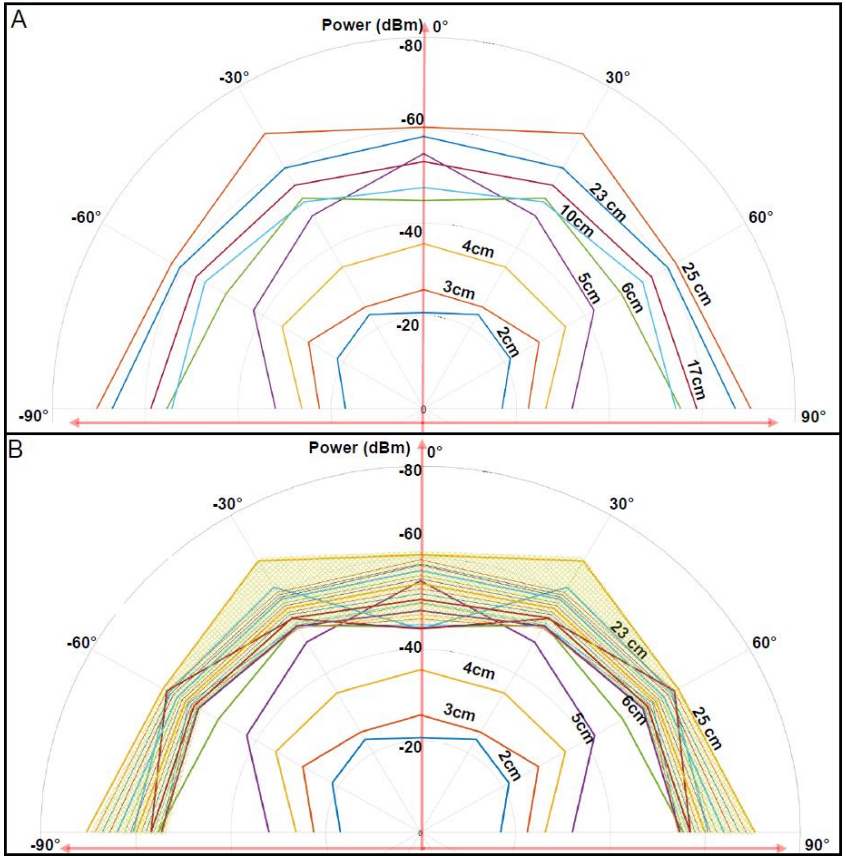

The Angular Analysis in Underground

- The angular analysis demonstrates that the magnetic field radiated at **13.56** MHz can be detected **Omnidirectionally.**

- The FracBot MCU requires **0.5s** to execute all reading tasks and transmission. This task requires **15mW** of the energy storage system.

- The received power in the region of **6-25 cm** is around **-50 dBm with compact antenna (30x40mm) and the transceiver output power of +20dBm (100mW).**

- This energy **(-50 dBm)** is enough to power-up the microcontroller for a simple temperature acquisition and data store.

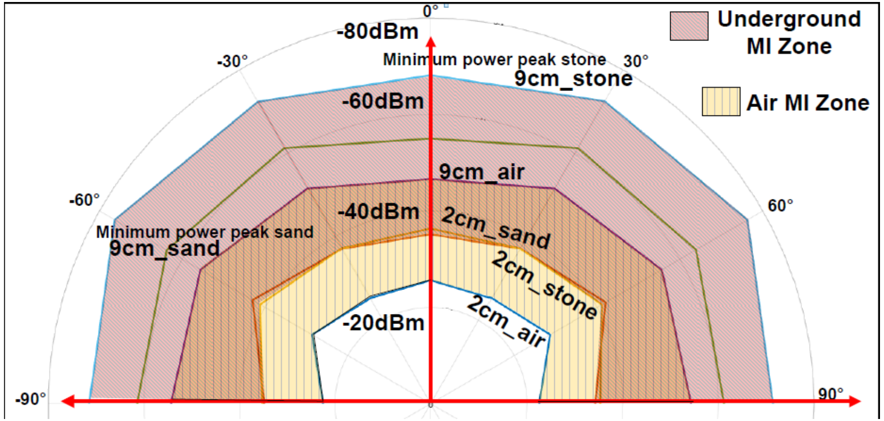

- The harvesting energy circuit (BQ25570) can not harvest and store energy for MI signal strength lower than **-30 dBm (1µW).**

- A nano harvesting circuit (<**1µW)** with ultra low sensitive receiver can allow the FracBot operation with signal strength of -**70 dBm.**

FracBot Gen II Development

FracBot Gen I → Design Optimization

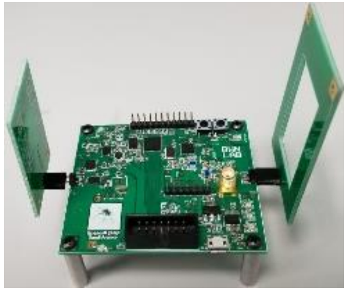

- Ultra-low-power electronics
- Processing & microcontroller
- Efficient communication
- Energy-harvesting capability
- Advanced Antenna Design

Advanced Microcontroller

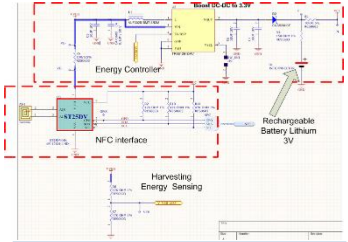

- Energy Unit Optimization
- Advanced NFC Transceiver

FracBot Gen II

Firmware Retransformation

FracBot Development

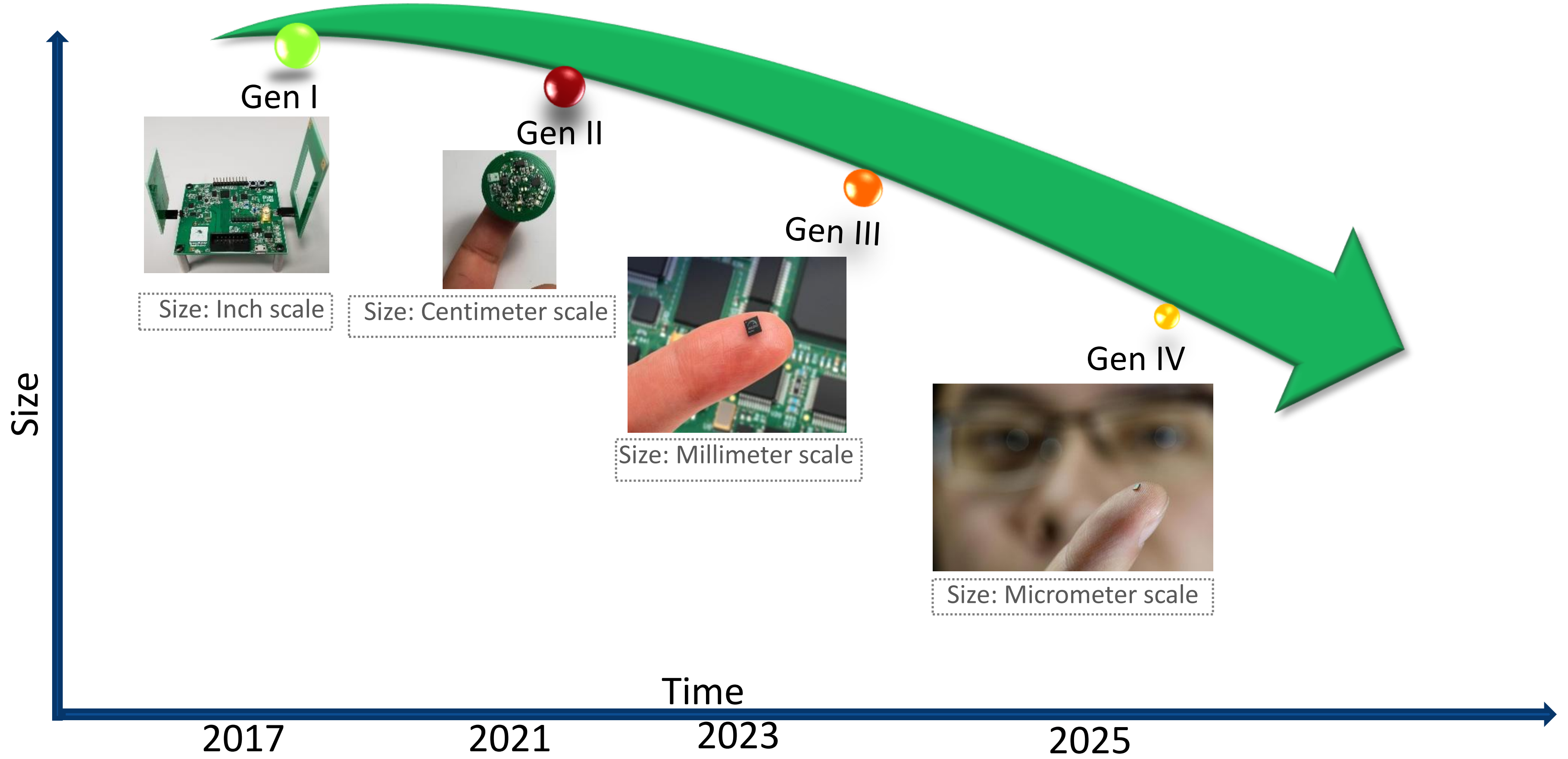

Conclusion

- Three key functions have been formulated and developed.
- A novel cross-layer communication framework for MI-based FracBot networks is developed to enable the communication in dynamically changing underground environments.
- A novel MI-based localization algorithms is developed to build up 3D constellation maps of hydraulic fracture.
- An energy model framework for a linear FracBot network topology is developed to estimates FracBot data transmission rates while respecting harvested energy constraints.
- A Novel prototypes of MI-based wireless FracBots are designed and developed.
- Designed for potential use as a platform for a new generation of WUSNs for monitoring hydraulic fractures and unconventional reservoirs, and measuring other wellbore parameters.
- Developed the hardware of the MI-based wireless FracBots for short-range communication using near-field communication (NFC) as a physical layer combined with an energy-harvesting capability and ultra-low power requirements.
- The hardware development and the testbed analyses allow us to better understand the environment challenges, improve the electronic sensitivity and optimize the minimum resources that are necessary to miniaturize the FracBot hardware.

Thank You

أرامكو السعودية
saudi aramco